Journal Pre-proof

Discovery of AdipoRon analogues as novel AMPK activators without inhibiting mitochondrial complex I

Geng Sun, Yanping You, Haobin Li, Yalong Cheng, Ming Qian, Xinyu Zhou, Haoliang Yuan, Qing-Long Xu, Liang Dai, Pengfei Wang, Keguang Cheng, Xiaoan Wen, Caiping Chen

PII: S0223-5234(20)30437-2

DOI: https://doi.org/10.1016/j.ejmech.2020.112466

Reference: EJMECH 112466

To appear in: *European Journal of Medicinal Chemistry*

Received Date: 15 January 2020

Revised Date: 12 May 2020

Accepted Date: 13 May 2020

Please cite this article as: G. Sun, Y. You, H. Li, Y. Cheng, M. Qian, X. Zhou, H. Yuan, Q.-L. Xu, L. Dai, P. Wang, K. Cheng, X. Wen, C. Chen, Discovery of AdipoRon analogues as novel AMPK activators without inhibiting mitochondrial complex I, *European Journal of Medicinal Chemistry* (2020), doi: https://doi.org/10.1016/j.ejmech.2020.112466.

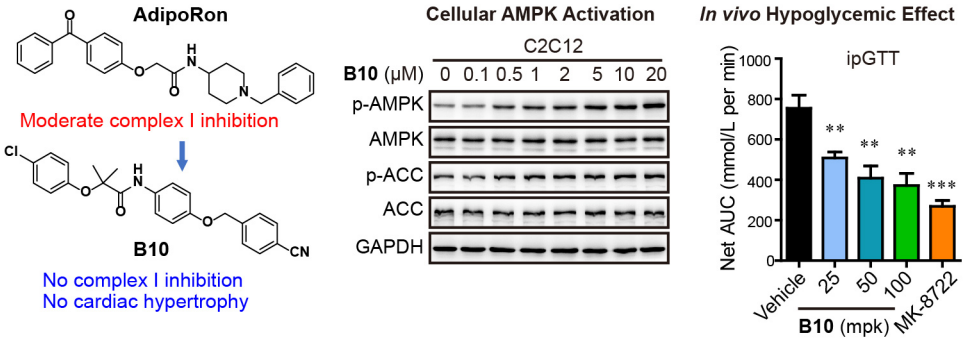

Discovery of AdipoRon analogues as novel AMPK activators without inhibiting mitochondrial complex I

Geng Sun [a,†], Yanping You [a,†], Haobin Li [a], Yalong Cheng [a], Ming Qian [a], Xinyu Zhou [a], Haoliang Yuan [a], Qing-Long Xu [a], Liang Dai [a], Pengfei Wang [a], Keguang Cheng [b], Xiaoan Wen [a,*], Caiping Chen [a,*]

[a] *Jiangsu Key Laboratory of Drug Discovery for Metabolic Disease, State Key Laboratory of Natural Medicines, China Pharmaceutical University, Nanjing 210009, China*

[b] *State Key Laboratory for the Chemistry and Molecular Engineering of Medicinal Resources, School of Chemistry and Pharmacy of Guangxi Normal University, Guilin 541004, China*

[†] These authors contributed equally to this article.

[*] Corresponding authors: Tel/fax: +86-25-83271150. E-mail: caiping.chen@cpu.edu.cn (C. P. Chen); wxagj@126.com (X. A. Wen)

Keywords

AMPK, activator, AdipoRon, Complex I, hypoglycemic action

Abstract

Activation of AMPK emerges as a potential therapeutic approach to metabolic diseases. AdipoRon is claimed to be an adiponectin receptor agonist that activates AMPK through adiponectin receptor 1 (AdipoR1). However, AdipoRon also exhibits moderate inhibition of mitochondrial complex I, leading to increased risk of lactic acidosis. In order to find novel AdipoRon analogues that activate AMPK without inhibition of complex I, 27 analogues of AdipoRon were designed, synthesized and biologically evaluated. As results, benzyloxy arylamide **B10** was identified as a potent AMPK activator without inhibition of complex I. **B10** dose-dependently improved glucose tolerance in normal mice, and significantly lowered fasting blood glucose level and ameliorated insulin resistance in db/db diabetic mice. More importantly, unlike the pan-AMPK activator MK-8722, **B10** did not cause cardiac hypertrophy, probably owing to its selective activation of AMPK in the muscle tissue but not in the heart tissue. Together, **B10** represents a novel class of AMPK activators with promising therapeutic potential against metabolic disease.

1. Introduction

Adenosine monophosphate-activated protein kinase (AMPK) is a master sensor of energy state and nutrient supply [1, 2]. It serves as a heterotrimeric serine/threonine protein kinase. Composed of a catalytic subunit α (α1 or α2) and two regulatory subunits β (β1 or β2) and γ (γ1, γ2 or γ3), AMPK theoretically creates 12 heterotrimeric isoforms that exhibit distinct tissue distribution and function in mammals [3]. Physiologically, AMPK is mainly activated through α-subunit Thr172 phosphorylation by the upstream kinases liver kinase B1 (LKB1) and Ca^{2+}/calmodulin-dependent protein kinase kinase β (CaMKKβ) [4-6]. It has been reported that the Thr172 phosphorylation increased the kinase activity of AMPK by >100 fold [7, 8]. In addition, allosteric activation also plays an important role in AMPK activation during energy stress [7, 9].

AMPK activation functions allowing for modulating energy balance, turning on catabolic pathways for ATP generation and switching off biosynthetic pathways for

energy conservation by phosphorylation of downstream target proteins. For instance, AMPK activation promotes insulin-independent glucose uptake to generate ATP in skeletal muscle, decreases gluconeogenesis and fatty acid synthesis in liver, and reduces fatty acid synthesis in adipose tissue [10, 11]. Therefore, AMPK emerges as an attractive target for treatment of type 2 diabetes mellitus (T2DM) and other metabolic diseases. Two types of anti-diabetic drugs, metformin [12, 13] and thiazolidinediones (TZDs) [14], have been proved to exert hypoglycemic effect at least partly through indirect activation of AMPK.

Various structural types of small molecule direct activators have been reported, including AICAR (Fig. 1) that entered clinical trials but was abandoned due to side effects. Several bottleneck problems arise with the current direct activators. For examples, AICAR as an AMP analogue *in vivo* could affect other AMP-dependent enzymes in addition to targeting AMPK, thus generating AMPK-independent effects [15]. PF-249 (Fig. 1), specifically acting on AMPK β1 isoform, did not result in acute glucose-lowering effect since the skeletal muscle mainly expresses AMPK β2 isoform [16]. As a potent pan-AMPK activator, MK-8722 (Fig. 1) could cause cardiac hypertrophy, although it greatly improved glucose homeostasis [17].

On the other hand, many indirect AMPK activators have been identified. For example, R419 (Fig. 1) is one of the most potent indirect AMPK activators that works through inhibiting mitochondrial respiratory complex I to elevate cellular AMP:ATP ratio [18, 19]. AMPK activation by metformin [20], TZDs [21] and berberine [11, 22] is also believed to be achieved through inhibition of complex I. Together, indirect AMPK activation through inhibiting mitochondrial complex I would increase the risk of lactic acidosis risk [10, 23]. This is evidenced by the result from a phase I trial of R118 (a close derivative of R419), showing that inhibition of mitochondrial complex I by R118 led to severe lactic acidosis in all the subjects at the highest dose [24].

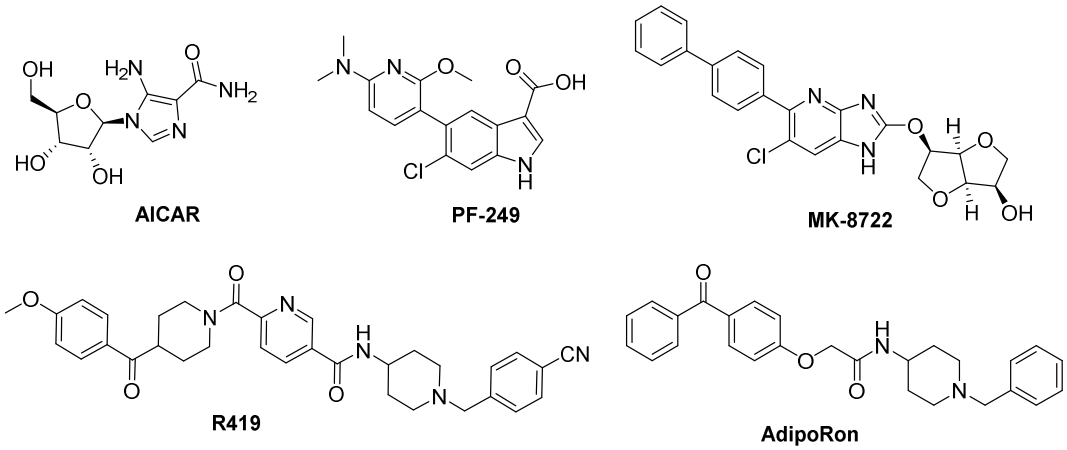

Fig. 1 The structures of some AMPK activators

Adiponectin is one of the most abundant adipokines, which exerts insulin sensitizing and anti-inflammatory effects through adiponectin receptors 1 and 2 (AdipoR1 and AdipoR2), leading to activation of AMPK and PPARα pathways, respectively [25-27]. Therefore, agonism of AdipoR1 might represent an indirect manner to activate AMPK. There are several peptide AdipoR agonists identified [28]. In 2013, Okada-Iwabu *et al.* reported a small molecule AdipoR agonist AdipoRon, which significantly ameliorated glucose intolerance and insulin resistance in mice through activating AMPK (EC_{50} about 10 μM) [29, 30]. AdipoRon has attracted much attention, and by far more than 50 articles have been published with using AdipoRon as a tool compound for biological and therapeutic proof-of-concept studies. Nevertheless, in 2018, Akimoto *et al.* disclosed that AdipoRon could also cause cellular complex I inhibition and mitochondrial dysfunction [31]. During our studies on the structural modifications on AdipoRon, we found that AdipoRon indeed inhibited mitochondrial respiratory chain (data not shown). Beyond AdipoRon, very few other small molecule AdipoR agonists have been reported by far [32].

In this study, we aimed to develop novel AdipoRon analogues as AMPK activators without inhibiting mitochondrial complex I. As shown in Fig. 2, AdipoRon shares high structural similarity with the complex I inhibitor R419, and thus we tried to substantially reduce this similarity. In this regard, two series of AdipoRon analogues (**A1~A15**, **B1~B12**) were designed (Fig. 2). In series A, the direction of 4-aminopiperidinyl moiety was inverted and the 4-amino was derivatized to

phenylureas. In series B, 4-aminophenoxy moiety was used instead of 4-aminopiperidinyl. Moreover, in both series of compounds, chloride was chosen to replace the phenyl ketone, a potential metabolic site of AdipoRon, and gem-dimethyl were introduced at the α-position of amide to further add metabolic stability. After synthesis and biological evaluation of these analogues, several potent AMPK activators were discovered. Among them, compound **B10** showed significant *in vitro* and *in vivo* hypoglycemic effects. More importantly, it had no complex I inhibitory activity and did not cause cardiac hypertrophy.

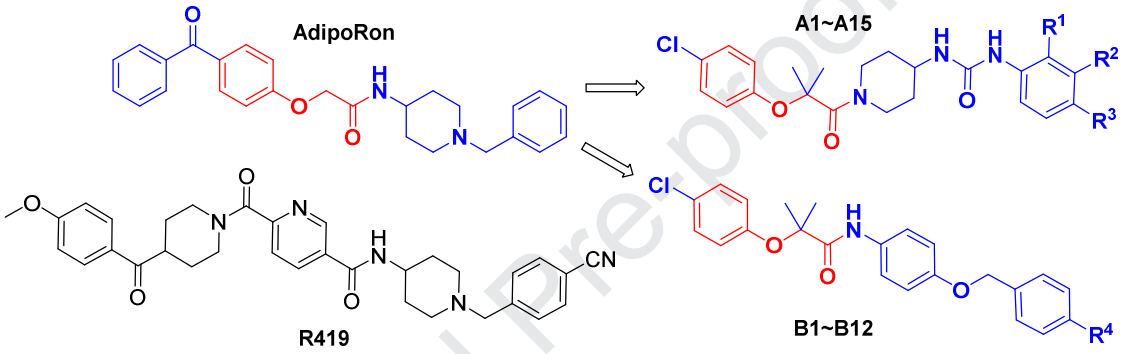

Fig. 2 Design of AdipoRon analogues

2. Results and discussion

2.1 Synthesis of AdipoRon analogues

The general synthetic route to analogues **A1~A15** is shown in Scheme 1. 2-(4-chlorophenoxy)-2-methylpropanoic acid was successively treated by oxalyl chloride and *tert*-butyl piperidin-4-yl carbamate to give the amide **2**, which was Boc-deprotected by HCl to give 4-amino-piperidine salt **3**. Phenyl carbonochloridate was condensed with various anilines to give the carbamates **1a~1k**. Finally, **3** underwent nucleophilic substitution reactions with **1a~1k** or various isocyanatobenzenes to afford analogues **A1~A15**.

Scheme 1. General synthetic route to the analogues **A1~A15**

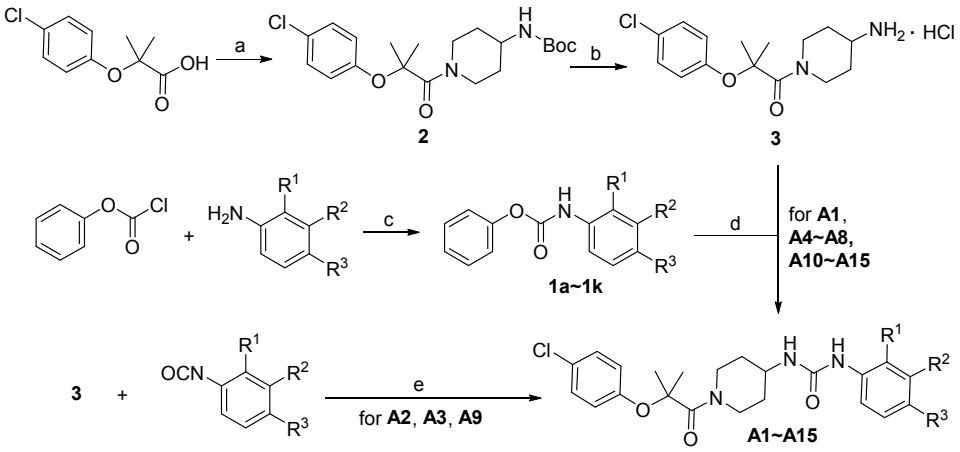

Reagents and conditions: (a) $(COCl)_2$, DMF, DCM, 0 ^oC to r.t., 3 h; then *tert*-butyl piperidin-4-ylcarbamate, DIPEA, 0 ^oC to r.t., 1 h, 86%; (b) HCl, EtOAc, r.t., overnight, 92%; (c) TEA, DCM, r.t., 3 h, 49-75%; (d) TEA, DMSO, r.t., 4 h, 34-80%; (e) TEA, DCM, r.t., 4 h, 44-60%.

Scheme 2. General synthetic route to the analogues **B1~B12**

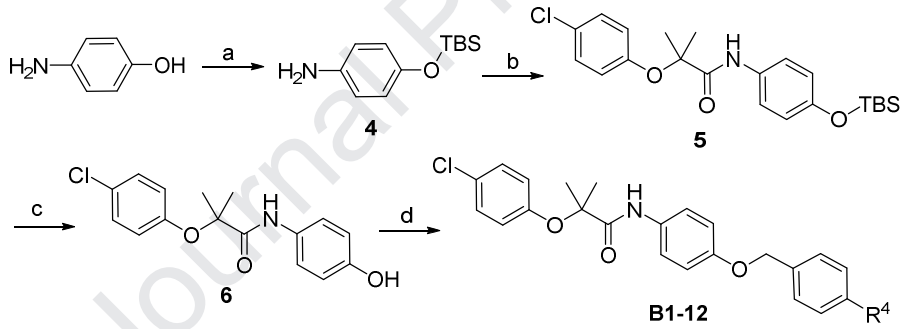

Reagents and conditions: (a) TBSCl, Imidazole, DCM, 0 ^oC to r.t. 1 h; (b) 2-(4-chlorophenoxy)-2-methylpropanoic acid, $(COCl)_2$, DMF, DCM, 0 ^oC to r.t., 3 h; then TEA, DCM, 0 ^oC to r.t., 1 h, 56% for two steps; (c) TEA·3HF, DCM, r.t., 10 h, 82%; (d) substituted benzyl halides, K_2CO_3, DMF, 65 ^oC, 27-81%.

Analogues **B1~B12** were synthesized according to the route shown in Scheme 2. 4-Aminophenol was protected by TBS to form the silicon ether **4**. 2-(4-Chlorophenoxy)-2-methylpropanoic acid was successively treated by oxalyl chloride and aniline **4** to give amide **5**, which was then TBS-deprotected by TEA·3HF and finally etherified with substituted benzyl halides to afford **B1~B12**.

2.2 Screening for AMPK phosphorylation by the compounds

All the 27 analogues were evaluated by Western blotting for their effects on phosphorylation of AMPK Thr172. Screening was performed in mouse C2C12 myotube cells at 10 μM of compounds. The results (Fig. 3) showed that 20 compounds increased phosphorylation of AMPK by more than 50%. Among them, six compounds (**A2**, **A3**, **A6**, **B2**, **B10** and **B11**) were much more potent than AdipoRon and comparable to MK-8722.

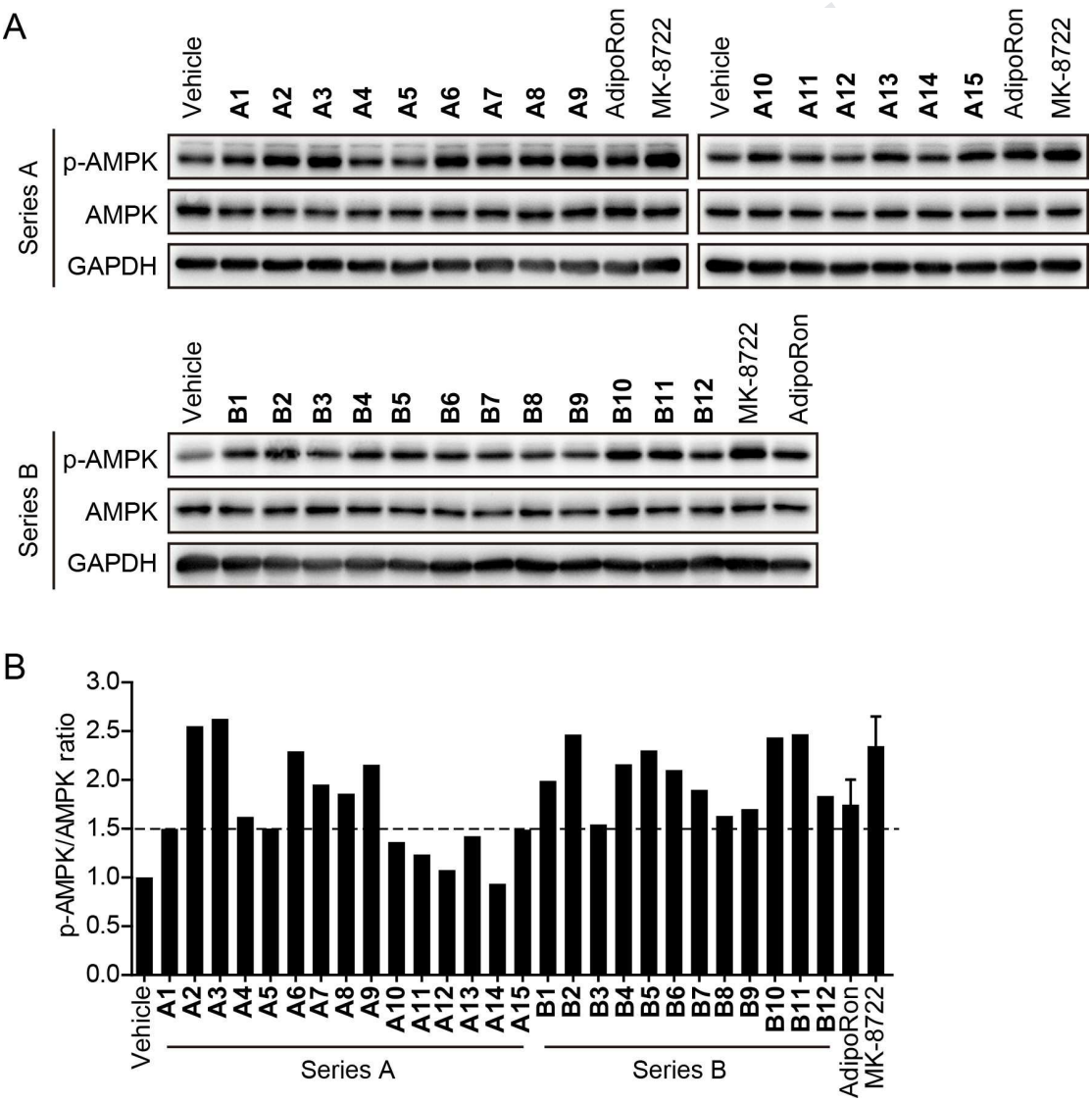

Fig. 3 Phosphorylation of AMPK in C2C12 myotube cells. (A) p-AMPK and AMPK were analyzed by Western blot assay in C2C12 myotubes treated for 2 h with compounds (10 μM). (B) Ratios of p-AMPK/AMPK were quantified. The values were represented as folds of the DMSO vehicle group.

2.3 Glucose consumption in C2C12 myotube cells

Skeletal muscle is the primary tissue to dispose glucose and lower glucose levels upon activation of AMPK [16]. Therefore, all the 27 analogues were evaluated for their effects on glucose consumption in mouse C2C12 myotube cells at a concentration of 10 μM. As shown in Table 1, among the A-series analogues, **A6** (R^3 = CF_3) and **A11** (R^3 = OMe) stimulated a 34~37% increase in glucose consumption, comparable to the effect of AdipoRon, while other compounds in the A-series had weak or no activity.

Table 1 Glucose consumption stimulated by **A1~A15** in C2C12 myotube cells.

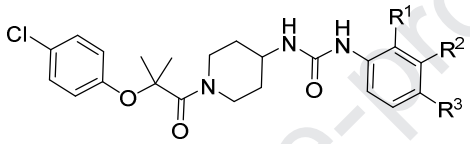

Compd.	R^1	R^2	R^3	GC (%) [a]
A1	H	H	H	118.0±14.7
A2	H	H	F	119.3±6.5
A3	H	H	Cl	104.1±10.9
A4	H	H	Br	127.3±12.9
A5	H	Cl	F	116.7±16.3
A6	H	H	CF_3	137.2±17.6
A7	H	CF_3	H	91.0±12.4
A8	CF_3	H	H	116.1±18.5
A9	H	H	OCF_3	104.2±11.2
A10	H	H	Me	93.7±4.3
A11	H	H	OMe	134.4±14.1
A12	H	H	COOEt	126.1±6.1

A13	H	H	COOH	117.7±4.7
A14	H	H	CN	116.2±14.6
A15	H	H	NO_2	115.4±12.8
AdipoRon				132.4±13.6
DMSO				100

[a] Glucose consumption (GC) relative to the DMSO group. All compounds were tested at 10 μM.

In the B-series of compounds, three compounds (**B4**, **B10** and **B11**) were remarkably more potent than AdipoRon and two compounds (**B6** and **B7**) were comparable to the effect of AdipoRon (Table 2). Several electron-withdrawing groups were favorable for R^4 in stimulating glucose consumption. Compounds **B4**, **B10** and **B11**, respectively bearing CF_3, CN and SO_2Me, showed the best potency with GC increasing 44~56%. By contrast, compounds **B6** (R^4 = OMe) and **B7** (R^4 = OCF_3) had much decreased potency, and compound **B5** (R^4 = Me) showed almost no activity.

Table 2. Glucose consumption stimulated by **B1-B15** in C2C12 myotube cells.

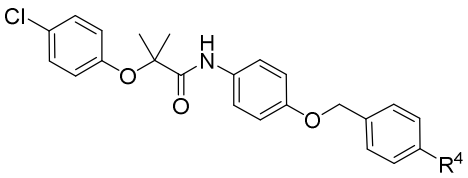

Compd.	R^4	GC (%)[a]
B1	F	107.6±12.2
B2	Cl	129.0±11.4
B3	Br	112.7±10.9
B4	CF_3	156.1±14.9
B5	Me	102.2±28.3

B6	OMe	134.7±8.1
B7	OCF_3	133.4±23.0
B8	COOMe	124.7±11.4
B9	COOH	116.5±6.7
B10	CN	151.8±4.0
B11	SO_2Me	144.4±12.9
B12	*t*-Bu	105.3±19.7
AdipoRon		132.4±13.6
DMSO		100

[a] Glucose consumption (GC) relative to the DMSO group. All compounds were tested at 10 μM.

2.4 Further confirmation of the AMPK activation effects of B10

Since compound **B10** showed strong activity both in AMPK activation screening and glucose consumption assays, further validation of its AMPK activation effects was performed.

Acetyl-CoA carboxylase (ACC), a key substrate of AMPK, is commonly used as the marker of AMPK activation. As shown in Fig. 4A, compound **B10** induced dose-dependently phosphorylation of ACC in C2C12 myotube cells, and the phosphorylation of ACC was highly consistent with the phosphorylation of AMPK. Time course experiments revealed that AMPK activation was significant after 1 h of compound **B10** treatment, reached to a high level after 6 h and maintained high within 6-24 h (Fig. 4B). Besides, **B10** also increased the phosphorylation of AMPK and ACC in human hepatocarcinoma HepG2 and HuH-7 cells, though the potency was a little less than that in C2C12 cells (Fig. 4C-F). All these data confirmed that compound **B10** was a potent AMPK activator.

Preliminary mechanism study proposed that **B10** activated AMPK probably in an indirect manner since in the enzymatic tests, **B10** had no influence on the enzymatic

activity of AMPK α1β1γ1 (widely distributed) and α2β2γ1 (predominant in skeletal muscle) (Fig. S1).

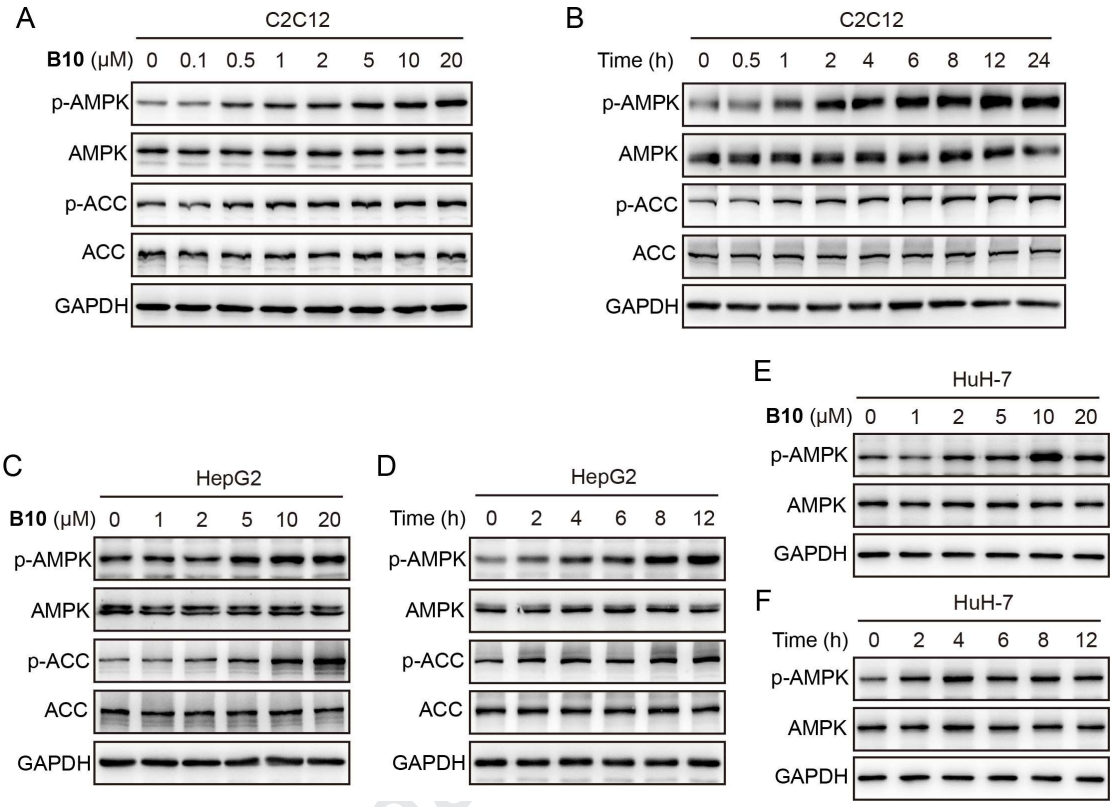

Fig. 4 Compound **B10** induced phosphorylation of AMPK and its downstream protein ACC. C2C12 myotubes (A and B), HepG2 (C and D) and HuH-7 (E and F) cells were treated with different concentrations of **B10** for 2 h or with a single dose of 10 μM for different time courses. The phosphorylation and total protein levels of cellular AMPK and ACC were analyzed by Western blotting.

2.5 B10 neither inhibits mitochondrial complex I nor elevates cellular AMP and ADP

It is well-known that elevation of cellular AMP:ATP and ADP:ATP ratios by complex I inhibition leads to activation of AMPK. Recently, AdipoRon was reported to inhibit cellular complex I activity and cause mitochondrial dysfunction [31], which is contradictory to the previous report by Kadowaki's group [29]. Notably, we also found that AdipoRon indeed inhibited mitochondrial respiratory chain at 10 μM (data not shown). Taken together, AdipoRon could increase the risk of lactic acidosis.

To our delight, compounds **B10** and **A6** did not inhibit complex I at 5~20 μM concentrations, while **B4** showed a significant inhibition of complex I (Fig. 5A). Effects of **B10** on cellular AMP and ADP levels were then examined. Consistently, compound **B10** did not increase the ratios of ADP/ATP and AMP/ATP in HepG2 cell, while the positive control R419 robustly increased these two ratios (Fig. 5B and C). Together, these results demonstrated that AMPK activation by **B10** was not through elevating cellular AMP and ADP levels.

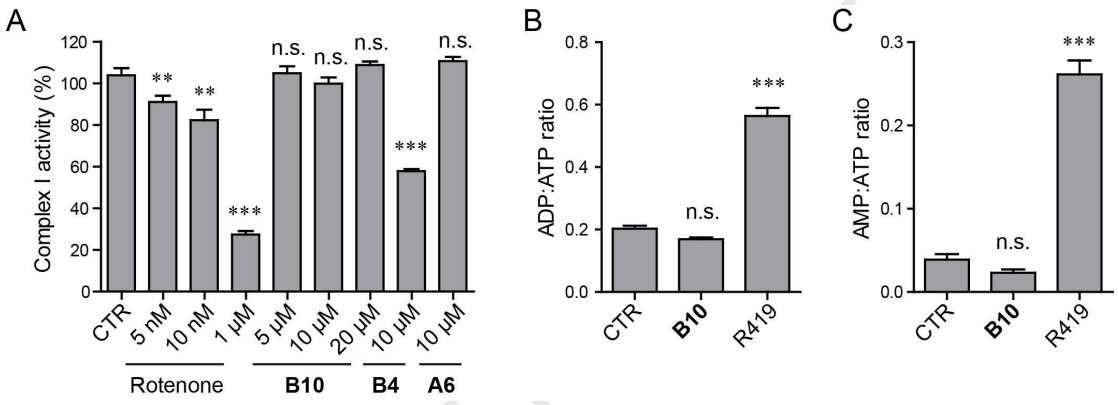

Fig. 5 Effects of **B10**, **B4** and **A6** on complex I activity or ratios of AMP/ADP to ATP. (A) Effects of **B10**, **B4** and **A6** on mitochondrial complex I activity. Rotenone was served as positive control. (B) Ratio of cellular ADP:ATP in HepG2 cells treated with **B10** (10 μM) or R419 (0.5 μM) or DMSO control (CTR). (C) Ratio of cellular AMP:ATP in HepG2 cells treated as (B). Data are expressed as mean ± S.D. for 3 replicates. ***P* <0.01, ****P* <0.001; relative to CTR; as determined by Student's *t* test. n.s., not significant.

2.6 B10-mediated AMPK phosphorylation requires LKB1

We therefore hypothesized that **B10** might induce AMPK phosphorylation through activation of the upstream signaling pathway. LKB1 and CaMKKβ are the two upstream kinases of AMPK. To clarify whether one or both of these kinases were required for the AMPK phosphorylation by **B10**, LKB1 was first knocked down by siRNA in C2C12 cells (Fig. S2A). As a result, LKB1 knockdown dramatically blocked the **B10**-stimulated phosphorylation of AMPK and ACC (Fig. S2B). Then, two human lung epithelial cell lines, BEAS-2B (LKB1 wild-type) and A549 (LKB1 mutant, CaMKKβ expressing), were subjected to **B10** treatment. The results showed that **B10** activated AMPK in the BEAS-2B cells, but not in the A549 cells (Fig. S2C).

As expected, the positive control MK-8722 was still efficient in the A549 cells (Fig. S2C), because it activated AMPK by both allosteric enhancement of the catalytic activity and prevention of Thr172 from dephosphorylation [17, 33]. Next, CaMKKβ in the C2C12 cells was inhibited using STO-609. As a result, the effect of CaMKKβ inhibition was negligible on the **B10-**induced AMPK phosphorylation (Fig. S2D). All of these demonstrated that AMPK activation by **B10** was LKB1 dependent. Further studies are ongoing to reveal the detailed mechanisms.

2.7 Effect of B10 on cell viability

Prior to *in vivo* studies, cytotoxicity of compound **B10** was examined in C2C12 cells, HepG2 cells and A549 cells by MTT assay. As shown in Fig. 6, no significant influence was observed for **B10** on the cell viability of C2C12 cells and A549 cells at the tested concentrations, and only slight decrease in the viability of HepG2 cells was detected after 72 h of treatment at 10 μM and 20 μM.

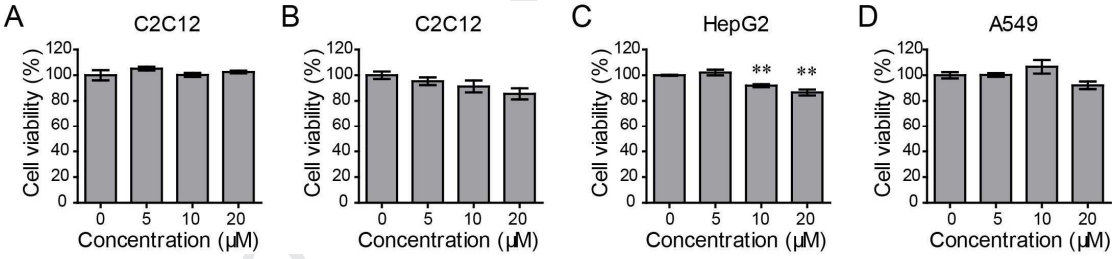

Fig. 6 Effect of **B10** on the cell viability. Cell viability was determined by MTT assay in C2C12 (A and B), HepG2 (C) and A549 cells (D) treated with **B10** for 24 h (A) or 72 h (B-D). Each group had 3 replicates. ***P* <0.001 vs 0 μM group (Student's *t* test).

2.8 Metabolic stability profiles of B10 and B4 in liver microsomes

In vitro metabolic stability profiles of compounds **B10** and **B4** were measured in human and mouse liver microsomes, with Ketanserin as control to validate the assay. As shown in Table 3, both **B10** and **B4** were fairly stable against human liver microsome metabolism, with 74% and 93% remaining at 45 min, respectively, and $T_{1/2}$ values of 97 min and >120 min, respectively. When exposed to mouse liver microsomes, **B4** also displayed a good stability, while **B10** showed a moderate stability with 39% remaining at 45 min and a $T_{1/2}$ value of 36 min.

Table 3. Metabolic stability profiles of **B10** and **B4**.

Compd.	Human liver microsomes			Mouse liver microsomes		
	Remaining at 45 min	$T_{1/2}$ (min)	Clint (mL/min/kg)	Remaining at 45 min	$T_{1/2}$ (min)	Clint (mL/min/kg)
B4	93%	>120	N/A[a]	91%	>120	N/A[a]
B10	74%	97	18	39%	36	152
Ketanserin	27%	25	71	21%	21	258

[a] not acquired.

As derivatives of para-aminophenol, compounds **B10** and **B4** had a potential to produce para-iminoquinone metabolites. However, this potential was probably limited by the steric hindrance of their benzyl groups, as the ethyl group in phenacetin successfully prevented the formation of para-iminoquinone metabolites [34].

2.9 *In vivo* hypoglycemic efficacy of B10

In vivo hypoglycemic efficacy of **B10** was then examined, since it showed promising *in vitro* properties. First, an intraperitoneal glucose tolerance test (ipGTT) was performed in normal lean C57BL/6 mice. As shown in Fig. 7A and B, compound **B10** dose-dependently improved glucose tolerance, although not as effective as the positive control MK-8722. Notably, at the same dose of 100 mg/kg, **B10** was a little more effective than AdipoRon in lowering blood glucose, but no statistical significance was observed (Fig. 7C and D).

Anti-hyperglycemic effect of **B10** was further assessed in diabetic db/db mice. Compared with vehicle control group, once-daily intragastrical administration of **B10** (100 mg/kg) for 2~6 weeks significantly lowered the fasting blood glucose in db/db mice (Fig. 7E). Moreover, **B10** treatment for 9 weeks significantly improved insulin resistance in db/db mice (Fig. 7F). During this long-term of treatment, the body weight and the serum levels of alanine aminotransferase (ALT) and aspartate aminotransferase (AST) (two markers of liver injury) were not significantly affected (Fig. 7G-I), indicating that **B10** at the tested dosages was relatively safe. **B10** treatment also seemed to have no improvement in lipid homeostasis, since the serum

levels of triglyceride (TG) and total cholesterol (TC) in the treatment group were comparable to those in the control group (Fig. S3).

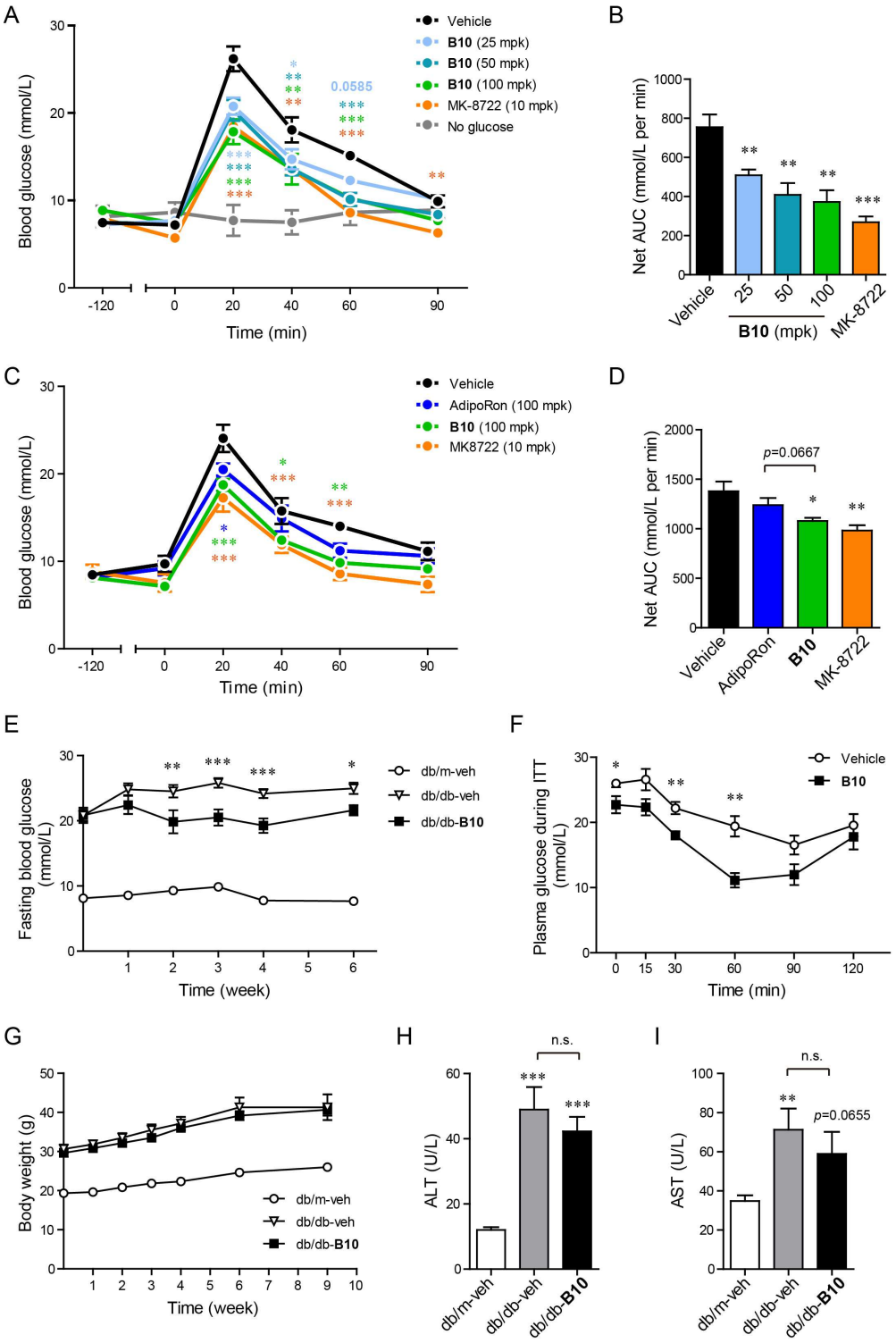

Fig. 7 B10 lowered plasma glucose and improved insulin resistance in mice. (A-B) Effects of acute **B10** administration (25, 50 and 100 mg/kg) in an ipGTT in C57BL/6 mice (8-to

10-week-old male, n=6 per group). (B) Net area under curve (AUC) of the data in (A). (C) ipGTT in C57BL/6 mice receiving **B10** (100 mg/kg), AdipoRon (100 mg/kg), MK-8722 (10 mg/kg) or vehicle. (D) Net area under curve (AUC) of the data in (C). (E) Fasting blood glucose levels were analyzed in db/db mice receiving **B10** (100 mg/kg) (db/db-**B10**) or vehicle (db/db-veh) and db/m mice (nondiabetic control) receiving vehicle (db/m-veh) at the indicated weeks of treatment. (F) Plasma glucose during insulin tolerance test (ITT) (1.5U insulin per kg body weight) in db/db mice treated with or without **B10** (100 mg/kg) for 9 weeks. (G) Body weights of mice at the indicated weeks of treatment of **B10** (100 mg/kg) or vehicle. (H and I) Serum levels of ALT (H) and AST (I) from mice receiving **B10** (100 mg/kg) or vehicle for 10 weeks. Data are expressed as mean ± SEM. *$p < 0.05$, **$p < 0.01$ and ***$p < 0.001$ compared with vehicle group (A-D) or db/db-veh group (E and F) or db/m-veh group (H and I), two-way ANOVA (A, C, E and F) or Student's *t* test (B, D, H and I).

2.10 B10 does not cause cardiac hypertrophy

One of the major concerns with AMPK activators is the risk of cardiac side effects. Gain-of-function mutations in *PRKAG2* gene (encoding AMPK γ2 subunit) can cause hypertrophic cardiomyopathy and an increase in cardiac glycogen. Notably, a similar phenotype appeared in animals treated by the pan-AMPK activator MK-8722 [17]. We therefore examined whether **B10** could cause hypertrophic effect in mice heart. As shown in Fig. 8A-D, unlike MK-8722, 4-week administration of compound **B10** did not cause cardiac hypertrophy nor increased cardiac glycogen in normal lean C57BL/6 mice. No obvious changes were detected in gross morphology of heart, heart weight/body weight ratio and heart weight/tibia length ratio. **B10** treatment for 10 weeks did not either induce cardiac hypertrophy or glycogen accumulation in diabetic db/db mice (Fig. S4). The heart and skeleton muscle tissues from **B10**-treated normal lean C57BL/6 mice were subjected to comparative analysis of AMPK activation. Interestingly, unlike MK-8722, **B10** did not increase the levels of p-AMPK or p-ACC in heart tissues (Fig. 8E), but elevated skeletal muscle p-ACC, albeit not as potent as MK-8722 (Fig. 8F). AMPK activation by **B10** was further determined in a rat cardiac cell line H9C2. Similarly, **B10** was much less efficient to stimulate the

phosphorylation of AMPK and ACC in cardiac H9C2 cells, compared with its effect in C2C12 myotube cells (Fig. 8G and H). All these results suggested that compound **B10** might be selective for muscle over heart tissues in term of AMPK activation, thus avoiding the risk of cardiac hypertrophy.

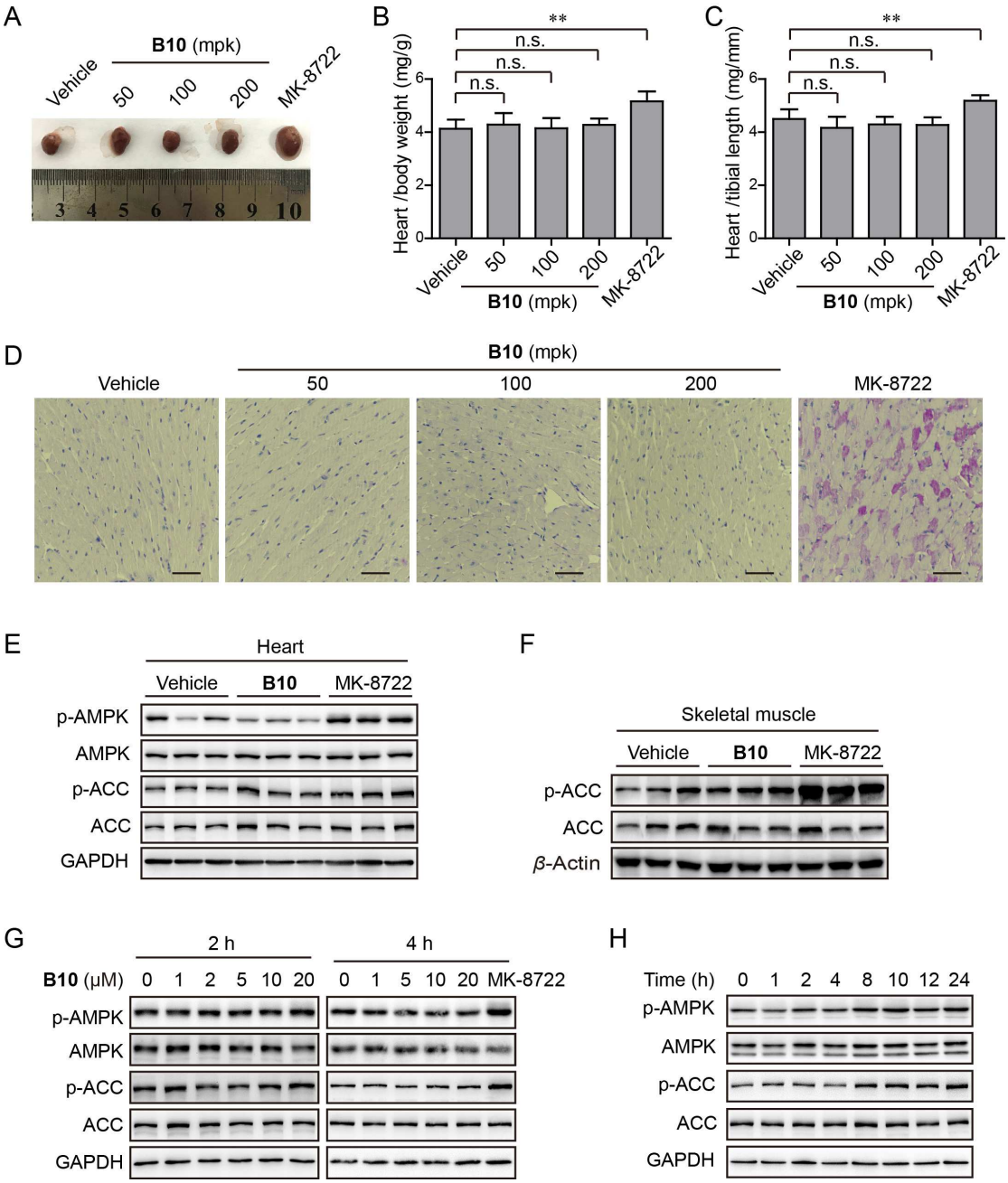

Fig. 8 Effect of chronic **B10** treatment on cardiac parameters in mice. (A) Gross morphology of hearts from mice administrated with **B10** (50, 100 and 200 mg/kg), MK-8722 (10 mg/kg) and vehicle control for 4 weeks (6 mice each group). (B-D) Effects of **B10** administration on heart weight/body weight ratio (B), heart weight/tibia length ratio (C) and cardiac glycogen (D). Scale

bar: 50 μm. (E and F) p-AMPK and p-ACC in heart (E) and skeletal muscle (F) were analyzed by Western blot assay after administration with **B10** or MK-8722 or vehicle. (G-H) Western blot analysis of phosphorylation and total amounts of AMPK and ACC in H9C2 cells after treatment with concentrations of **B10** for 2 h or 4 h (G) or with a single concentration at 10 μM for a time course (H). $^{**}p < 0.01$ compared with the vehicle group.

3. Conclusion

In this study, 27 analogues of AdipoRon have been designed and synthesized. Among them, six compounds (**A2**, **A3**, **A6**, **B2**, **B10** and **B11**) were found to activate AMPK much more potently than AdipoRon in C2C12 myotubes, and two compounds (**B4** and **B10**) exhibited superior activity in stimulating glucose consumption (GC > 150%). Cellular AMP/ADP analysis and *in vitro* enzymatic test demonstrated that **B10** did not inhibit mitochondrial complex I. Experiments with LKB1 knockdown and mutant cells revealed that the **B10**-mediated AMPK phosphorylation required the upstream kinase LKB1. *In vivo* study results showed that oral administration of **B10** dose-dependently improved glucose tolerance in normal mice, and significantly lowered fasting blood glucose level and ameliorated insulin resistance in db/db diabetic mice at the doses of 25~100 mg/kg/day. More importantly, unlike the pan-AMPK activator MK-8722, **B10** did not cause cardiac hypertrophy and glycogen accumulation. It was revealed that **B10** selectively activated AMPK in the muscle tissues, but not in the heart tissues. Taken together, **B10** represents a novel class of AMPK activators that hold therapeutic promise for metabolic diseases.

4. Experimental section

4.1 Chemistry

General information General procedures of the synthesis route were described as below. Commercially available reagents and solvents were used without further purification. Analytical thin-layer chromatography (TLC) was performed on silica gel 60 F254 plates (Qingdao Ocean Chemical Company, China). Column chromatography was carried out on silica gel (200–300 mesh, Qingdao Ocean

Chemical Company, China). Nuclear magnetic resonance (NMR) spectra were performed on an ACF* 300Q Bruker spectrometer. Proton coupling patterns were described as singlet (s), doublet (d), doublet of doublets (dd), triplet (t), triplet of doublets (td), quartet (q), multiplet (m), and broad (br). Low- and high-resolution mass spectra (MS and HRMS) were given with electrospray ionization (ESI) produced by Waters Q-TOF Micro and Agilent G6230B, respectively. Melting points (mp) were measured in open capillary tubes, using an RY-1G melting point apparatus (0 to 300 °C).

All target compounds were confirmed with over 95% purity by Agilent Prime LC with a detector 1260 DAD HS at 220 nm and a column Agilent Poroshell HPH-C18 (2.1 × 50 mm, 2.7 μm). Water containing 0.1% formic acid (A) and acetonitrile containing 0.05% formic acid (B) were used to perform elution at a flow rate of 1.2 mL/min, with a gradient from 30 to 95% B (or 50 to 100% B) over 4.5 min and 95% B (or 100% B) held for 0.5 min (see Supporting Information, Table S1).

General procedures for synthesis of **A1**~**A15** and **B1~B12** are examplified by **A1**/**A2** and **B1**, respectively. Experimental details for synthesis of **1a~1k** and **2~6** are included in Supporting information.

4.1.1 1-(1-(2-(4-Chlorophenoxy)-2-methylpropanoyl)piperidin-4-yl)-3-phenylurea (**A1**)

Phenyl phenylcarbamate (**1a**) (70 mg, 0.33 mmol) was added to a solution of **3** (100 mg, 0.3 mmol) and TEA (83 μL, 0.6 mmol) in DMSO (4 mL). The reaction mixture was stirred at room temperature for 4 h, poured into ice water with stirring and filtered. The collected crude product was suspended in anhydrous Et_2O (4 mL), stirred and filtered to yield compound **A1** (100 mg, 80%) as a white solid. mp: 176-178 ^{o}C. ^{1}H NMR (300 MHz, DMSO-d_6) δ ppm 8.20 (s, 1 H), 7.39-7.29 (m, 4 H), 7.24-7.14 (m, 2 H), 6.92-6.78 (m, 3 H), 6.06 (d, J = 7.5 Hz, 1 H), 4.39-4.15 (m, 2 H), 3.69-3.56 (m, 1 H), 3.27-3.13 (m, 1 H), 2.98-2.82 (m, 1 H), 1.89-1.61 (m, 2 H), 1.55 (s, 6 H), 1.20-1.09 (m, 1 H), 0.97-0.80 (m, 1 H). ^{13}C NMR (75 MHz, DMSO-d_6) δ ppm 169.69, 154.28, 153.98, 140.24, 129.20, 128.48, 125.11, 120.92, 118.58, 117.50, 80.71, 45.79,

43.63, 41.37, 32.18, 31.94, 25.79, 25.35. ESI-MS: *m/z* 438.2 $[M+Na]^+$. HRMS (ESI): *m/z* calcd for $C_{22}H_{27}ClN_3O_3$ $[M+H]^+$ 416.1735, found 416.1738. LC t_R: 1.991 min, purity 99.21%.

4.1.2

1-(1-(2-(4-chlorophenoxy)-2-methylpropanoyl)piperidin-4-yl)-3-(4-fluorophenyl)urea (**A2**)

1-fluoro-4-isocyanatobenzene (41 mg, 0.3 mmol) was added to a solution of **3** (100 mg, 0.3 mmol) and TEA (83 µL, 0.6 mmol) in CH_2Cl_2 (4 mL). The reaction mixture was stirred at room temperature for 4 h before water was added. The solution was extracted with CH_2Cl_2 (2 x 8 mL) and the organic layer was washed with brine, dried over Na_2SO_4, filtered, and concentrated. The crude product was purified by column chromatography (CH_2Cl_2/ethyl acetate = 5/1) and the residue was suspended in hexane (4 mL), stirred and filtered to yield compound **A2** (70 mg, 54%) as a white solid. mp: 186-189 ^oC. ^1H NMR (300 MHz, DMSO-d_6) δ ppm 8.24 (s, 1 H), 7.39-7.30 (m, 4 H), 7.03 (dd, *J* = 8.9, 8.9 Hz, 2 H), 6.82 (d, *J* = 8.9 Hz, 2 H), 6.06 (d, *J* = 7.5 Hz, 1 H), 4.40-4.15 (m, 2 H), 3.69-3.53 (m, 1 H), 3.28-3.14 (m, 1 H), 3.00-2.81 (m, 1 H), 1.89-1.61 (m, 2 H), 1.55 (s, 6 H), 1.26-1.09 (m, 1 H), 0.98-0.77 (m, 1 H). ^{13}C NMR (75 MHz, DMSO-d_6) δ ppm 169.69, 156.80 (d, *J* = 237.2 Hz), 154.34, 153.98, 136.60 (d, *J* = 2.3 Hz), 129.21, 125.11, 119.11 (d, *J* = 7.6 Hz), 118.58, 114.93 (d, *J* = 22.1 Hz), 80.71, 45.84, 43.61, 41.34, 32.17, 31.93, 25.85, 25.37. ESI-MS: *m/z* 456.2 $[M+Na]^+$. HRMS (ESI): *m/z* calcd for $C_{22}H_{26}ClFN_3O_3$ $[M+H]^+$ 434.1641, found 434.1645. LC t_R: 2.105 min, purity 99.96%.

4.1.3

1-(1-(2-(4-chlorophenoxy)-2-methylpropanoyl)piperidin-4-yl)-3-(4-chlorophenyl)urea (**A3**)

White solid, yield 44%. mp: 155-157 ^oC. ^1H NMR (300 MHz, DMSO-d_6) δ ppm 8.35 (s, 1 H), 7.37 (d, *J* = 8.8 Hz, 2 H), 7.34 (d, *J* = 8.8 Hz, 2 H),7.23 (d, *J* = 8.8 Hz, 2 H), 6.82 (d, *J* = 8.9 Hz, 2 H), 6.12 (d, *J* = 7.4 Hz, 1 H), 4.40-4.15 (m, 2 H), 3.70-3.59

(m, 1 H), 3.27-3.12 (m, 1 H), 3.01-2.76 (m, 1 H), 1.90-1.62 (m, 2 H), 1.55 (s, 6 H), 1.27-1.09 (m, 1 H), 1.04-0.79 (m, 1 H). ^{13}C NMR (75 MHz, DMSO-d_6) δ ppm 169.70, 154.13, 153.98, 139.24, 129.20, 128.31, 125.12, 124.44, 118.99, 118.58, 80.71, 45.86, 43.61, 41.32, 32.10, 31.83, 25.79, 25.36. ESI-MS: *m/z* 448.1 $[M-H]^-$. HRMS (ESI): *m/z* calcd for $C_{22}H_{26}Cl_2N_3O_3$ $[M+H]^+$ 450.1346, found 450.1353. LC t_R: 2.478 min, purity 99.95%.

4.1.4

1-(4-bromophenyl)-3-(1-(2-(4-chlorophenoxy)-2-methylpropanoyl)piperidin-4-yl)urea (**A4**)

White solid, yield 41%. mp: 176-178 °C. ^{1}H NMR (300 MHz, DMSO-d_6) δ ppm 8.36 (s, 1 H), 7.41-7.27 (m, 6 H), 6.82 (d, *J* = 9.0 Hz, 2 H), 6.13 (d, *J* = 7.4 Hz, 1 H), 4.40-4.18 (m, 2 H), 3.69-3.56 (m, 1 H), 3.26-3.15 (m, 1 H), 2.98-2.84 (m, 1 H), 1.87-1.63 (m, 2 H), 1.55 (s, 6 H), 1.25-1.09 (m, 1 H), 0.99-0.80 (m, 1 H). ^{13}C NMR (75 MHz, DMSO-d_6) δ ppm 169.69, 154.08, 153.97, 139.66, 131.21, 129.21, 125.11, 119.42, 118.58, 112.21, 80.71, 45.85, 43.60, 41.40, 32.13, 31.88, 25.80, 25.41. ESI-MS: *m/z* 516.1 $[M+Na]^+$. HRMS (ESI): *m/z* calcd for $C_{22}H_{26}BrClN_3O_3$ $[M+H]^+$ 494.0841 and 496.0820, found 494.0841 and 496.0819. LC t_R: 2.583 min, purity 99.73%.

4.1.5

1-(3-chloro-4-fluorophenyl)-3-(1-(2-(4-chlorophenoxy)-2-methylpropanoyl)piperidin-4-yl)urea (**A5**)

White solid, yield 70%. mp: 167-169 °C. ^{1}H NMR (300 MHz, DMSO-d_6) δ ppm 8.42 (s, 1 H), 7.71 (dd, *J* = 6.8, 2.5 Hz, 1 H), 7.34 (d, *J* = 8.9 Hz, 2 H), 7.24 (dd, *J* = 9.0, 9.0 Hz, 1H), 7.20-7.12 (m, 1H), 6.82 (d, *J* = 8.9 Hz, 2 H), 6.18 (d, *J* = 7.4 Hz, 1 H), 4.40-4.17 (m, 2 H), 3.69-3.57 (m, 1 H), 3.25-3.15 (m, 1 H), 2.97-2.81 (m, 1 H), 1.88-1.63 (m, 2 H), 1.55 (s, 6 H), 1.21-1.09 (m, 1 H), 0.99-0.84 (m, 1 H). ^{13}C NMR (75 MHz, DMSO-d_6) δ ppm 169.70, 154.13, 153.97, 151.79 (d, *J* = 240.1 Hz), 137.55 (d, *J* = 2.7 Hz), 129.20, 125.12, 118.89 (d, *J* = 18.3 Hz), 118.72, 118.58, 117.63 (d, *J*

= 6.6 Hz), 116.52 (d, *J* = 21.6 Hz), 80.71, 45.97, 43.58, 41.38, 32.13, 31.82, 25.78, 25.41. ESI-MS: *m/z* 490.1 $[M+Na]^+$. HRMS (ESI): *m/z* calcd for $C_{22}H_{25}Cl_2FN_3O_3$ $[M+H]^+$ 468.1252, found 468.1253. LC t_R: 2.590 min, purity 99.86%.

4.1.6

1-(1-(2-(4-chlorophenoxy)-2-methylpropanoyl)piperidin-4-yl)-3-(4-(trifluoromethyl)phenyl)urea (**A6**)

White solid, yield 45%. mp: 169-171 °C. ^{1}H NMR (300 MHz, DMSO-d_6) δ ppm 8.66 (s, 1 H), 7.60-7.49 (m, 4 H), 7.35 (d, *J* = 8.9 Hz, 2 H), 6.82 (d, *J* = 8.9 Hz, 2 H), 6.25 (d, *J* = 7.4 Hz, 1 H), 4.43-4.17 (m, 2 H), 3.75-3.60 (m, 1 H), 3.29-3.13 (m, 1 H), 2.99-2.80 (m, 1 H), 1.9-1.62 (m, 2 H), 1.55 (s, 6 H), 1.28-1.09 (m, 1 H), 1.08-0.83 (m, 1 H). ^{13}C NMR (75 MHz, DMSO-d_6) δ ppm 169.71, 153.98, 153.91, 143.94, 129.21, 125.79 (q, *J* = 3.8 Hz), 125.13, 124.51 (q, *J* = 270.9 Hz), 120.97 (q, *J* = 31.8 Hz), 118.59, 117.12, 80.71, 45.92, 43.64, 41.35, 32.09, 31.78, 25.79, 25.31. ESI-MS: *m/z* 506.2 $[M+Na]^+$. HRMS (ESI): *m/z* calcd for $C_{23}H_{26}ClF_3N_3O_3$ $[M+H]^+$ 484.1609, found 484.1607. LC t_R: 2.865 min, purity 98.96%.

4.1.7

1-(1-(2-(4-chlorophenoxy)-2-methylpropanoyl)piperidin-4-yl)-3-(3-(trifluoromethyl)phenyl)urea (**A7**)

White solid, yield 34%. mp: 80-83°C. ^{1}H NMR (300 MHz, DMSO-d_6) δ ppm 8.60 (s, 1 H), 7.93 (s, 1 H), 7.48-7.40 (m, 2 H), 7.35 (d, *J* = 8.9 Hz, 2 H), 7.26-7.16 (m, 1 H), 6.82 (d, *J* = 8.9 Hz, 2 H), 6.23 (d, *J* = 7.4 Hz, 1 H), 4.41-4.17 (m, 2 H), 3.72-3.57 (m, 1 H), 3.27-3.14 (m, 1 H), 2.97-2.81 (m, 1 H), 1.90-1.63 (m, 2 H), 1.55 (s, 6 H), 1.24-1.10 (m, 1 H), 1.01-0.84 (m, 1 H). ^{13}C NMR (75 MHz, DMSO-d_6) δ ppm 169.75, 154.18, 154.00, 141.10, 129.59, 129.39 (q, *J* = 31.1 Hz), 129.23, 125.16, 124.16 (d, *J* = 272.1 Hz), 121.06, 118.62, 117.18 (d, *J* = 3.6 Hz), 113.50 (q, *J* = 4.0 Hz), 80.74, 46.01, 43.68, 41.43, 32.04, 31.76, 25.78, 25.37. ESI-MS: *m/z* 506.2 $[M+Na]^+$. HRMS (ESI): *m/z* calcd for $C_{23}H_{26}ClF_3N_3O_3$ $[M+H]^+$ 484.1609, found 484.1613. LC t_R: 2.743 min, purity 99.98%.

4.1.8

1-(1-(2-(4-chlorophenoxy)-2-methylpropanoyl)piperidin-4-yl)-3-(2-(trifluoromethyl)phenyl)urea (**A8**)

White solid, yield 61%. mp: 138-140 °C. ^{1}H NMR (300 MHz, DMSO-d_6) δ ppm 7.96 (d, *J* = 8.4 Hz, 1 H), 7.65-7.50 (m, 3 H), 7.35 (d, *J* = 8.9 Hz, 2 H), 7.20-7.11 (m, 1 H), 6.98 (d, *J* = 7.2 Hz, 1 H), 6.83 (d, *J* = 8.9 Hz, 2 H), 4.36-4.15 (m, 2 H), 3.70-3.59 (m, 1 H), 3.28-3.17 (m, 1 H), 3.01-2.88 (m, 1 H), 1.89-1.63 (m, 2 H), 1.55 (s, 6 H), 1.25-1.11 (m, 1 H), 0.99-0.84 (m, 1 H). ^{13}C NMR (75 MHz, DMSO-d_6) δ ppm 169.73, 153.99, 137.21, 132.60, 129.24, 125.61 (q, *J* = 5.1 Hz), 125.14, 124.12, 124.00 (d, *J* = 272.7 Hz), 122.33, 118.59, 118.23 (q, *J* = 29.0 Hz), 80.72, 46.08, 43.57, 41.30, 32.11, 31.79, 25.86, 25.37. ESI-MS: *m/z* 506.2 $[M+Na]^+$. HRMS (ESI): *m/z* calcd for $C_{23}H_{26}ClF_3N_3O_3$ $[M+H]^+$ 484.1609, found 484.1616. LC t_R: 2.521 min, purity 99.85%.

4.1.9 1-(1-(2-(4-chlorophenoxy)-2-methylpropanoyl) piperidin-4-yl)-3-(4-(trifluoromethoxy) phenyl) urea (**A9**)

White solid, yield 60%. mp: 96-98 °C. ^{1}H NMR (300 MHz, DMSO-d_6) δ ppm 8.43 (s, 1 H), 7.43 (d, *J* = 9.1 Hz, 2 H), 7.35 (d, *J* = 9.0 Hz, 2 H), 7.20 (d, *J* = 8.6 Hz, 2 H), 6.82 (d, *J* = 9.0 Hz, 2 H), 6.14 (d, *J* = 7.4 Hz, 1 H), 4.37-4.19 (m, 2 H), 3.70-3.56 (m, 1 H), 3.28-3.15 (m, 1 H), 3.00-2.82 (m, 1 H), 1.87-1.61 (m, 2 H), 1.55 (s, 6 H), 1.20-1.08 (m, 1 H), 0.97-0.82 (m, 1 H). ^{13}C NMR (75 MHz, DMSO-d_6) δ ppm 169.89, 154.33, 154.10, 142.14, 139.61, 129.36, 125.26, 121.57, 120.23 (q, *J* = 255.1 Hz), 118.75, 118.72, 80.84, 46.03, 43.77, 41.48, 32.35, 31.87, 25.98, 25.42. ESI-MS: *m/z* 522.2 $[M+Na]^+$. HRMS (ESI): *m/z* calcd for $C_{23}H_{26}ClF_3N_3O_4$ $[M+H]^+$ 500.1558, found 500.1557. LC t_R: 2.794 min, purity 99.87%.

4.1.10 1-(1-(2-(4-chlorophenoxy)-2-methylpropanoyl)piperidin-4-yl)-3-(p-tolyl)urea (**A10**)

White solid, yield 54%. mp: 168-171 °C. ^{1}H NMR (300 MHz, DMSO-d_6) δ ppm 8.09 (s, 1 H), 7.34 (d, *J* = 8.4 Hz, 2 H), 7.21 (d, *J* = 7.8 Hz, 2 H), 6.99 (d, *J* = 7.8 Hz,

2 H), 6.82 (d, *J* = 8.5 Hz, 2 H), 6.01 (d, *J* = 6.9 Hz, 1 H), 4.39-4.15 (m, 2 H), 3.70-3.53 (m, 1 H), 3.28-3.14 (m, 1 H), 2.98-2.82 (m, 1 H), 2.19 (s, 3 H), 1.88-1.62 (m, 2 H), 1.55 (s, 6 H), 1.24-1.05 (m, 1 H), 0.97-0.76 (m, 1 H). ^{13}C NMR (75 MHz, DMSO-d_6) δ ppm 169.69, 154.28, 153.98, 140.24, 129.20, 128.48, 125.11, 120.92, 118.58, 117.50, 80.71, 45.79, 43.63, 41.37, 32.18, 31.94, 25.79, 25.35, 20.20. ESI-MS: *m/z* 452.2 $[M+Na]^+$. HRMS (ESI): *m/z* calcd for $C_{23}H_{29}ClN_3O_3$ $[M+H]^+$ 430.1892, found 430.1893. LC t_R: 2.299 min, purity 99.95%.

4.1.11

1-(1-(2-(4-chlorophenoxy)-2-methylpropanoyl)piperidin-4-yl)-3-(4-methoxyphenyl)urea (**A11**)

White solid, yield 67%. mp: 189-192 °C. ^{1}H NMR (300 MHz, DMSO-d_6) δ ppm 8.01 (s, 1 H), 7.34 (d, *J* = 8.8 Hz, 2 H), 7.23 (d, *J* = 8.8 Hz, 2 H), 6.82 (d, *J* = 9.5 Hz, 2 H), 6.79 (d, *J* = 9.4 Hz, 2 H), 5.95 (d, *J* = 7.3 Hz, 1 H), 4.38-4.17 (m, 2 H), 3.68 (s, 3 H), 3.64-3.53 (m, 1 H), 3.26-3.13 (m, 1 H), 2.98-2.81 (m, 1 H), 1.89-1.62 (m, 2 H), 1.55 (s, 6 H), 1.21-1.08 (m, 1 H), 0.95-0.79 (m, 1 H). ^{13}C NMR (75 MHz, DMSO-d_6) δ ppm 169.68, 154.52, 153.98, 153.88, 133.39, 129.20, 125.11, 119.25, 118.58, 113.80, 80.71, 55.06, 45.81, 43.64, 41.41, 32.30, 32.02, 25.75, 25.45. ESI-MS: *m/z* 468.2 $[M+Na]^+$. HRMS (ESI): *m/z* calcd for $C_{23}H_{29}ClN_3O_4$ $[M+H]^+$ 446.1841, found 446.1840. LC t_R: 1.931 min, purity 99.90%.

4.1.12 ethyl 4-(3-(1-(2-(4-chlorophenoxy)-2-methylpropanoyl)piperidin-4-yl)ureido)benzoate (**A12**)

White solid, yield 48%. mp: 127-129 °C. ^{1}H NMR (300 MHz, DMSO-d_6) δ ppm 8.65 (s, 1 H), 7.81 (d, *J* = 8.7 Hz, 2 H), 7.46 (d, *J* = 8.7 Hz, 2 H), 7.34 (d, *J* = 8.9 Hz, 2 H), 6.82 (d, *J* = 8.9 Hz, 2 H), 6.25 (d, *J* = 7.4 Hz, 1 H), 4.39-4.19 (m, 2 H), 4.25 (q, *J* = 7.1 Hz, 2 H), 3.74-3.59 (m, 1 H), 3.26-3.14 (m, 1 H), 2.99-2.83 (m, 1 H), 1.88-1.64 (m, 2 H), 1.55 (s, 6 H), 1.29 (t, *J* = 7.1 Hz, 3 H), 1.23-1.09 (m, 1 H), 1.02-0.83 (m, 1 H). ^{13}C NMR (75 MHz, DMSO-d_6) δ ppm 169.72, 165.36, 153.98,

153.82, 144.81, 130.16, 129.21, 125.13, 121.99, 118.59, 116.58, 80.72, 60.02, 45.92, 43.61, 41.37, 32.07, 31.72, 25.82, 25.48, 14.12. ESI-MS: *m/z* 510.2 $[M+Na]^+$. HRMS (ESI): *m/z* calcd for $C_{25}H_{31}ClN_3O_5$ $[M+H]^+$ 488.1947, found 488.1953. LC t_R: 2.491 min, purity 99.97%.

4.1.13

4-(3-(1-(2-(4-chlorophenoxy)-2-methylpropanoyl)piperidin-4-yl)ureido)benzoic acid (**A13**)

To a solution of **A12** (84 mg, 0.158 mmol) in THF (3 mL) and MeOH (2 mL) was added a solution of KOH (27 mg, 0.474 mmol) in H_2O (1 mL). The mixture was stirred at room temperature overnight and concentrated in vacuum. The residue was acidified to pH 2-3 by 1 N HCl, and filtered. The collected crude product was washed with CH_2Cl_2 and dried to yield compound **A13** (40 mg, 55%) as a white solid. mp: 178-180 ^oC. ^1H NMR (300 MHz, DMSO-d_6) δ ppm 12.48 (s, 1 H), 8.62 (s, 1 H), 7.79 (d, *J* = 8.3 Hz, 2 H), 7.44 (d, *J* = 8.4 Hz, 2 H), 7.35 (d, *J* = 8.6 Hz, 2 H), 6.82 (d, *J* = 8.6 Hz, 2 H), 6.25 (d, *J* = 7.1 Hz, 1 H), 4.40-4.15 (m, 2 H), 3.71-3.57 (m, 1 H), 3.27-3.14 (m, 1 H), 2.96-2.82 (m, 1 H), 1.90-1.62 (m, 2 H), 1.55 (s, 6 H), 1.26-1.08 (m, 1 H), 1.02-0.80 (m, 1 H). ^{13}C NMR (75 MHz, DMSO-d_6) δ ppm 169.73, 166.99, 154.01, 153.91, 144.54, 130.40, 129.28, 125.13, 122.86, 118.59, 116.52, 80.73, 45.92, 43.65, 41.35, 32.17, 31.77, 25.92, 25.33. ESI-MS: *m/z* 458.1 $[M-H]^-$. HRMS (ESI): *m/z* calcd for $C_{23}H_{27}ClN_3O_5$ $[M+H]^+$ 460.1634, found 460.1638. LC t_R: 1.554 min, purity 99.56%.

4.1.14

1-(1-(2-(4-chlorophenoxy)-2-methylpropanoyl)piperidin-4-yl)-3-(4-cyanophenyl)urea (**A14**)

White solid, yield 53%. mp: 183-185 ^oC. ^1H NMR (300 MHz, DMSO-d_6) δ ppm 8.76 (s, 1 H), 7.64 (d, *J* = 8.6 Hz, 2 H), 7.51 (d, *J* = 8.6 Hz, 2 H), 7.34 (d, *J* = 8.8 Hz, 2 H), 6.82 (d, *J* = 8.8 Hz, 2 H), 6.33 (d, *J* = 7.3 Hz, 1 H), 4.40-4.18 (m, 2 H), 3.74-3.59 (m, 1 H), 3.27-3.15 (m, 1 H), 2.98-2.80 (m, 1 H), 1.89-1.62 (m, 2 H), 1.55

(s, 6 H), 1.28-1.10 (m, 1 H), 1.04-0.82 (m, 1 H). ^{13}C NMR (75 MHz, DMSO-d_6) δ ppm 169.71, 153.97, 153.69, 144.67, 133.03, 129.22, 125.12, 119.26, 118.59, 117.34, 102.37, 80.72, 45.94, 43.66, 41.31, 31.97, 31.78, 25.72, 25.33. ESI-MS: *m/z* 463.2 $[M+Na]^+$. HRMS (ESI): *m/z* calcd for $C_{23}H_{26}ClN_4O_3$ $[M+H]^+$ 441.1688, found 441.1685. LC t_R: 2.172 min, purity 99.78%.

4.1.15

1-(1-(2-(4-chlorophenoxy)-2-methylpropanoyl)piperidin-4-yl)-3-(4-nitrophenyl)urea (**A15**)

White solid, yield 36%. mp: 179-182 ^{o}C. ^{1}H NMR (300 MHz, DMSO-d_6) δ ppm 9.02 (s, 1 H), 8.12 (d, *J* = 9.0 Hz, 2 H), 7.57 (d, *J* = 9.0 Hz, 2 H), 7.35 (d, *J* = 8.7 Hz, 2 H), 6.82 (d, *J* = 8.7 Hz, 2 H), 6.41 (d, *J* = 7.2 Hz, 1 H), 4.41-4.17 (m, 2 H), 3.76-3.57 (m, 1 H), 3.28-3.15 (m, 1 H), 3.01-2.82 (m, 1 H), 1.91-1.63 (m, 2 H), 1.55 (s, 6 H), 1.28-1.11 (m, 1 H), 1.01-0.84 (m, 1 H). ^{13}C NMR (75 MHz, DMSO-d_6) δ ppm 169.74, 154.00, 153.55, 146.91, 140.42, 129.28, 125.14, 125.04, 118.59, 116.75, 80.73, 46.08, 43.64, 41.32, 32.01, 31.62, 25.90, 25.32. ESI-MS: *m/z* 483.2 $[M+Na]^+$. HRMS (ESI): *m/z* calcd for $C_{22}H_{26}ClN_4O_5$ $[M+H]^+$ 461.1586, found 461.1581. LC t_R: 2.371 min, purity 99.82%.

4.1.16

2-(4-chlorophenoxy)-N-(4-((4-fluorobenzyl)oxy)phenyl)-2-methylpropanamide (**B1**)

A solution of 2-(4-chlorophenoxy)-N-(4-hydroxyphenyl)-2-methylpropanamide (**6**) (150 mg, 0.49 mmol), K_2CO_3 (136 mg, 0.98 mmol) and 1-(bromomethyl)-4-fluorobenzene (74 μL, 0.59 mmol) in DMF was stirred at 65 ^{o}C for 2 h. The reaction mixture was cooled to room temperature and acidified to pH 2-3 by 1 N HCl. The solution was extracted with EtOAc, washed with brine, dried over Na_2SO_4 and concentrated. The residue was purified by flash chromatography (petrol ether/ethyl acetate = 10/1) to give compound **B1** (120 mg, 59%) as a white solid. mp: 120-122 ^{o}C. ^{1}H NMR (300 MHz, DMSO-d_6) δ ppm 9.85 (s, 1 H), 7.54 (d, *J* = 9.0 Hz, 2 H), 7.48 (dd, *J* = 8.3, 5.8 Hz, 2 H), 7.34 (d, *J* = 8.9 Hz, 2 H), 7.20 (dd, *J* = 8.9, 8.9

Hz, 2 H), 6.95 (d, *J* = 9.1 Hz, 2 H), 6.94 (d, *J* = 8.9 Hz, 2 H), 5.05 (s, 2 H), 1.52 (s, 6 H). ^{13}C NMR (75 MHz, DMSO-d_6) δ ppm 171.66, 161.62 (d, *J* = 243.5 Hz), 154.51, 153.60, 133.31 (d, *J* = 2.9 Hz), 131.73, 129.68 (d, *J* = 8.3 Hz), 129.03, 126.15, 122.00, 121.38, 115.07 (d, *J* = 21.4 Hz), 114.64, 80.85, 68.60, 24.68. ESI-MS: *m/z* 436.2 $[M+Na]^+$. HRMS (ESI): *m/z* calcd for $C_{23}H_{22}ClFNO_3$ $[M+H]^+$ 414.1267, found 414.1268. LC t_R: 1.779 min, purity 99.80%.

4.1.17

N-(4-((4-chlorobenzyl)oxy)phenyl)-2-(4-chlorophenoxy)-2-methylpropanamide (**B2**)

White solid, yield 62%. mp: 120-123 °C. ^{1}H NMR (300 MHz, DMSO-d_6) δ ppm 9.86 (s, 1 H), 7.54 (d, *J* = 8.9 Hz, 2 H), 7.49-7.41 (m, 4 H), 7.34 (d, *J* = 8.8 Hz, 2 H), 6.94 (d, *J* = 9.0 Hz, 2 H), 6.93 (d, *J* = 8.8 Hz, 2 H), 5.07 (s, 2 H), 1.52 (s, 6 H). ^{13}C NMR (75 MHz, DMSO-d_6) δ ppm 171.66, 154.41, 153.59, 136.16, 132.23, 131.79, 129.25, 129.03, 128.28, 126.15, 122.00, 121.38, 114.65, 80.85, 68.47, 24.68. ESI-MS: *m/z* 452.1 $[M+Na]^+$. HRMS (ESI): *m/z* calcd for $C_{23}H_{22}Cl_2NO_3$ $[M+H]^+$ 430.0971, found 430.0971. LC t_R: 2.215 min, purity 99.48%.

4.1.18

N-(4-((4-bromobenzyl)oxy)phenyl)-2-(4-chlorophenoxy)-2-methylpropanamide (**B3**)

White solid, yield 27%. mp: 141-142 °C. ^{1}H NMR (300 MHz, DMSO-d_6) δ ppm 9.85 (s, 1 H), 7.58 (d, 8.7 Hz, 2 H), 7.54 (d, 9.7 Hz, 2 H), 7.39 (d, *J* = 8.2 Hz, 2 H), 7.34 (d, *J* = 8.7 Hz, 2 H), 7.00-6.87 (m, 4 H), 5.06 (s, 2 H), 1.52 (s, 6 H). ^{13}C NMR (75 MHz, DMSO-d_6) δ ppm 171.65, 154.38, 153.59, 136.59, 131.79, 131.20, 129.55, 129.02, 126.14, 121.99, 121.37, 120.71, 114.65, 80.84, 68.50, 24.68. ESI-MS: *m/z* 496.1 $[M+Na]^+$. HRMS (ESI): *m/z* calcd for $C_{23}H_{22}BrClNO_3$ $[M+H]^+$ 474.0466, found 476.0443. LC t_R: 2.334 min, purity 100%.

4.1.19

2-(4-chlorophenoxy)-2-methyl-N-(4-((4-(trifluoromethyl)benzyl)oxy)phenyl)propenamide (**B4**)

White solid, yield 65%. mp: 125-127 °C. ^{1}H NMR (300 MHz, DMSO-d_6) δ ppm

9.87 (s, 1 H), 7.75 (d, *J* = 7.9 Hz, 2 H), 7.65 (d, *J* = 7.8 Hz, 2 H), 7.56 (d, *J* = 8.7 Hz, 2 H), 7.33 (d, *J* = 8.7 Hz, 2 H), 6.97 (d, *J* = 9.0 Hz, 2 H), 6.94 (d, *J* = 8.9 Hz, 2 H), 5.20 (s, 2 H), 1.52 (s, 6 H). ^{13}C NMR (75 MHz, DMSO-d_6) δ ppm 171.73, 154.33, 153.61, 142.04, 131.91, 129.05, 128.21 (q, *J* = 31.6 Hz), 127.82, 126.17, 125.19 (q, *J* = 3.7 Hz), 124.16 (d, *J* = 272.0 Hz), 122.07, 121.41, 114.68, 80.87, 68.45, 24.70. ESI-MS: *m/z* 486.2 $[M+Na]^+$. HRMS (ESI): *m/z* calcd for $C_{24}H_{22}ClF_3NO_3$ $[M+H]^+$ 464.1235, found 464.1239. LC t_R: 2.415 min, purity 99.50%.

4.1.20

2-(4-chlorophenoxy)-2-methyl-N-(4-((4-methylbenzyl)oxy)phenyl)propenamide (**B5**)

White solid, yield 70%. mp: 100-102 °C. ^{1}H NMR (300 MHz, DMSO-d_6) δ ppm 9.84 (s, 1 H), 7.53 (d, *J* = 8.8 Hz, 2 H), 7.34 (d, *J* = 8.7 Hz, 2 H), 7.31 (d, *J* = 7.6 Hz, 2 H), 7.18 (d, *J* = 7.7 Hz, 2 H), 6.98-6.89 (m, 4 H), 5.01 (s, 2 H), 2.30 (s, 3 H), 1.52 (s, 6 H). ^{13}C NMR (75 MHz, DMSO-d_6) δ ppm 171.63, 154.65, 153.60, 136.84, 134.05, 131.59, 129.02, 128.81, 127.55, 126.14, 121.98, 121.38, 114.63, 80.85, 69.21, 24.68, 20.63. ESI-MS: *m/z* 408.2 $[M-H]^-$. HRMS (ESI): *m/z* calcd for $C_{24}H_{25}ClNO_3$ $[M+H]^+$ 410.1517, found 410.1524. LC t_R: 2.143 min, purity 99.65%.

4.1.21

2-(4-chlorophenoxy)-N-(4-((4-methoxybenzyl)oxy)phenyl)-2-methylpropanamide (**B6**)

White solid, yield 76%. mp: 126-129 °C. ^{1}H NMR (300 MHz, DMSO-d_6) δ ppm 9.84 (s, 1 H), 7.53 (d, *J* = 8.8 Hz, 2 H), 7.35 (d, *J* = 8.1 Hz, 2 H), 7.34 (d, *J* = 8.6 Hz, 2 H), 7.00-6.86 (m, 6 H), 4.98 (s, 2 H), 3.75 (s, 3 H), 1.52 (s, 6 H). ^{13}C NMR (75 MHz, DMSO-d_6) δ ppm 171.67, 158.89, 154.69, 153.64, 131.58, 129.31, 129.08, 128.98, 126.13, 121.98, 121.34, 114.65, 113.73, 80.86, 69.08, 55.03, 24.72. ESI-MS: *m/z* 424.2 $[M-H]^-$. HRMS (ESI): *m/z* calcd for $C_{24}H_{25}ClNO_4$ $[M+H]^+$ 426.1467, found 426.1470. LC t_R: 1.664 min, purity 99.88%.

4.1.22

2-(4-chlorophenoxy)-2-methyl-N-(4-((4-(trifluoromethoxy)benzyl)oxy)phenyl)propen

amide (**B7**)

White solid, yield 46%. mp: 94-96 °C. ^{1}H NMR (300 MHz, DMSO-d_6) δ ppm 9.86 (s, 1 H), 7.57 (d, *J* = 8.2 Hz, 2 H), 7.55 (d, *J* = 8.6 Hz, 2 H), 7.38 (d, *J* = 8.4 Hz, 2 H), 7.34 (d, *J* = 8.9 Hz, 2 H), 6.96 (d, *J* = 8.2 Hz, 2 H), 6.93 (d, *J* = 8.5 Hz, 2 H), 5.11 (s, 2 H), 1.52 (s, 6 H). ^{13}C NMR (75 MHz, DMSO-d_6) δ ppm 171.68, 154.43, 153.60, 147.76, 136.61, 131.83, 129.30, 129.02, 126.16, 122.02, 121.39, 120.83, 120.00 (q, *J* = 256.2 Hz), 114.62, 80.86, 68.38, 24.67. ESI-MS: *m/z* 478.2 $[M-H]^-$. HRMS (ESI): *m/z* calcd for $C_{24}H_{22}ClF_3NO_4$ $[M+H]^+$ 480.1184, found 480.1185. LC t_R: 2.474 min, purity 99.57%.

4.1.23 Methyl 4-((4-(2-(4-chlorophenoxy)-2-methylpropanamido)phenoxy)methyl)benzoate (**B8**)

White solid, yield 47 %. mp: 128-130 °C. ^{1}H NMR (300 MHz, DMSO-d_6) δ ppm 9.88 (s, 1 H), 7.98 (d, *J* = 8.2 Hz, 2 H), 7.57 (d, *J* = 8.0 Hz, 2 H), 7.55 (d, *J* = 8.9 Hz, 2 H),7.34 (d, *J* = 8.9 Hz, 2 H), 6.96 (d, *J* = 9.2 Hz, 2 H), 6.93 (d, *J* = 9.0 Hz, 2 H), 5.18 (s, 2 H), 3.85 (s, 3 H), 1.52 (s, 6 H). ^{13}C NMR (75 MHz, DMSO-d_6) δ ppm 171.67, 165.90, 154.37, 153.59, 142.68, 131.86, 129.18, 129.03, 128.87, 127.28, 126.14, 122.01, 121.37, 114.66, 80.85, 68.67, 51.97, 24.68. ESI-MS: *m/z* 476.2 $[M+Na]^+$. HRMS (ESI): *m/z* calcd for $C_{25}H_{25}ClNO_5$ $[M+H]^+$ 454.1416, found 454.1407. LC t_R: 1.659 min, purity 99.85%.

4.1.24 4-((4-(2-(4-chlorophenoxy)-2-methylpropanamido)phenoxy)methyl)benzoic acid (**B9**)

To a solution of **B8** (120 mg, 0.29 mmol) in MeOH (12 mL) was added $LiOH{\cdot}H_2O$ (48 mg, 1.1 mmol) in H_2O (3 mL). The mixture was stirred at room temperature overnight and concentrated. The residues was acidified to pH 2-3 with 1 N HCl. The solution was extracted with EtOAc, washed with brine, dried over Na_2SO_4 and concentrated. The residue was suspended in anhydrous Et_2O (4 mL) with stirring, and filtered to yield compound **B9** (110 mg, 95%) as a white solid. mp: 191-193 °C. ^{1}H NMR (300 MHz, DMSO-d_6) δ ppm 12.91 (s, 1 H), 9.87 (s, 1 H), 7.95 (d, *J* = 8.1 Hz,

2 H), 7.59-7.51 (m, 4 H), 7.34 (d, *J* = 8.8 Hz, 2 H), 6.96 (d, *J* = 8.7 Hz, 2 H), 6.93 (d, *J* = 8.7 Hz, 2 H), 5.17 (s, 2 H), 1.52 (s, 6 H). ^{13}C NMR (75 MHz, DMSO-d_6) δ ppm 171.72, 167.01, 154.43, 153.64, 142.21, 131.87, 130.09, 129.38, 129.10, 127.21, 126.15, 122.03, 121.35, 114.67, 80.86, 68.73, 24.72. ESI-MS: *m/z* 462.2 $[M+Na]^+$. HRMS (ESI): *m/z* calcd for $C_{24}H_{23}ClNO_5$ $[M+H]^+$ 440.1259, found 440.1262. LC t_R: 2.516 min, purity 99.36%.

4.1.25 2-(4-chlorophenoxy)-N-(4-((4-cyanobenzyl)oxy)phenyl)-2-methylpropanamide (**B10**)

White solid, yield 81%. mp: 124-126 ^{o}C. ^{1}H NMR (300 MHz, DMSO-d_6) δ ppm 9.87 (s, 1 H), 7.85 (d, *J* = 8.1 Hz, 2 H), 7.62 (d, *J* = 8.1 Hz, 2 H), 7.56 (d, *J* = 8.9 Hz, 2 H), 7.34 (d, *J* = 8.8 Hz, 2 H), 6.96 (d, *J* = 8.0 Hz, 2 H), 6.93 (d, *J* = 8.6 Hz, 2 H), 5.19 (s, 2 H), 1.52 (s, 6 H). ^{13}C NMR (75 MHz, DMSO-d_6) δ ppm 171.72, 154.20, 153.61, 142.97, 132.28, 131.97, 129.07, 127.90, 126.14, 122.03, 121.33, 118.65, 114.66, 110.36, 80.84, 68.35, 24.69. ESI-MS: *m/z* 443.1 $[M+Na]^+$. HRMS (ESI): *m/z* calcd for $C_{24}H_{22}ClN_2O_3$ $[M+H]^+$ 421.1313, found 421.1313. LC t_R: 3.076 min, purity 99.98%.

4.1.26 2-(4-chlorophenoxy)-2-methyl-N-(4-((4-(methylsulfonyl)benzyl)oxy)phenyl)propenamide (**B11**)

White solid, yield. mp: 145-146 ^{o}C ^{1}H NMR (300 MHz, DMSO-d_6) δ ppm 9.86 (s, 1 H), 7.94 (d, *J* = 8.2 Hz, 2 H), 7.69 (d, *J* = 8.2 Hz, 2 H), 7.55 (d, *J* = 8.9 Hz, 2 H), 7.34 (d, *J* = 8.9 Hz, 2 H), 6.97 (d, *J* = 9.2 Hz, 2 H), 6.94 (d, *J* = 9.0 Hz, 2 H), 5.22 (s, 2 H), 3.21 (s, 3 H), 1.52 (s, 6 H). ^{13}C NMR (75 MHz, DMSO-d_6) δ ppm 171.72, 154.24, 153.61, 143.20, 140.03, 131.93, 129.08, 127.86, 127.06, 126.11, 122.04, 121.31, 114.66, 80.83, 68.31, 43.48, 24.70. ESI-MS: *m/z* 474.1 $[M+H]^+$. HRMS (ESI): *m/z* calcd for $C_{24}H_{25}ClNO_5S$ $[M+H]^+$ 474.1136, found 474.1133. LC t_R: 2.573 min, purity 100%.

4.1.27

N-(4-((4-(tert-butyl)benzyl)oxy)phenyl)-2-(4-chlorophenoxy)-2-methylpropanamide (**B12**)

White solid, yield 43%. mp: 106-108 ^{o}C. ^{1}H NMR (300 MHz, DMSO-d_6) δ ppm 9.85 (s, 1 H), 7.54 (d, J = 8.9 Hz, 2 H), 7.43-7.30 (m, 6 H), 6.98-6.90 (m, 4 H), 5.03 (s, 2 H), 1.52 (s, 6 H), 1.28 (s, 9 H). ^{13}C NMR (75 MHz, DMSO-d_6) δ ppm 171.62, 154.69, 153.59, 150.12, 134.07, 131.58, 129.01, 127.35, 126.14, 124.99, 121.99, 121.38, 114.54, 80.85, 69.08, 34.13, 31.00, 24.68. ESI-MS: *m/z* 474.2 $[M+Na]^+$. HRMS (ESI): *m/z* calcd for $C_{27}H_{31}ClNO_3$ $[M+H]^+$ 452.1987, found 452.1986. LC t_R: 3.014 min, purity 99.93%.

4.2 Biology

Chemicals and Reagents Primary antibodies against AMPK (#2532), p-AMPK (#2535), ACC (#3676) and p-ACC (#3661) were purchased from Cell Signaling Technology. Anti-GAPDH antibody (ARG10112) was purchased from Arigo Biolaboratories. STO-609 were purchased from Merck. Rotenone were purchased from Energy Chemical Inc (Shanghai, China).

4.2.1 Cell culture

C2C12, HepG2, HuH-7, BEAS-2B and A549 cells were purchased from the Cell Bank of Shanghai Institute of Cell Biology, Chinese Academy of Sciences (Shanghai, China). The four human cell lines were verified by STR analysis, provided by the Cell Bank of Shanghai Institute of Cell Biology, Chinese Academy of Sciences and further confirmed by Guangzhou Cellcook Biotech Co., Ltd. (Guangzhou, China). C2C12, HepG2, HuH-7 and A549 cells were maintained in high glucose (4.5 g/L) Dulbecco's modified Eagle's medium (DMEM). BEAS-2B cells were maintained in RPMI 1640 medium. All the mediums were supplemented with 10% fetal bovine serum (FBS), penicillin (100 U/mL) and streptomycin (100 μg/mL) at 37 °C in humidified atmosphere containing 5% CO_2.

For C2C12 cell differentiation, cells were seeded at 2×10^5/well into 12-well plate in high glucose DMEM (10% FBS). After 24 h, cells were transferred to be

maintained in DMEM containing 2% horse serum for 5-7 days until the myotubes formed universally. The medium was refreshed every day during differentiation.

4.2.2 Western blot assay

After being treated with compounds, cells were gently washed with PBS twice and then lysed by RIPA buffer (150 mM NaCl, 1% NP-40, 0.5% sodium deoxycholate, 0.1% SDS, 50 mM Tris-HCl, pH 7.5) with protease and phosphatase inhibitor cocktails. For tissues, weighted skeletal muscles and hearts were homogenized in RIPA buffer containing protease and phosphatase inhibitors, and centrifuged at 10,600 g for 20 min. Equal amounts of protein (~30 μg per sample) were subjected to Western blot analysis as previously described [35, 36]. Briefly, the proteins were blotted to PVDF membranes. After being blocked with 5% bovine serum albumin, the membranes were incubated individually with primary antibody against AMPK, p-AMPK, ACC, p-ACC or internal control (GAPDH or *β*-Actin) at 4 °C overnight. The corresponding secondary antibodies conjugated with horseradish peroxidase (HRP) were added and the blots were visualized by using an enhanced chemiluminescence method. Luminescence was measured by a chemiluminescent imaging system (Tanon, Shanghai, China) and quantified using TanonImage software. The ratios of p-AMPK / AMPK were represented as folds of the vehicle group.

4.2.3 Glucose consumption assay

After C2C12 cell differentiation, the culture medium of the high glucose DMEM was replaced with DMEM containing 2.75 g/L glucose. Then cells were treated with compounds or DMSO control, and three cell-free blank wells were only filled with the same volume of medium. After 12 h of incubation, the culture medium was collected and centrifuged. The supernatant was subjected to the measurement of glucose level by using a glucose oxidase kit (E1010, Applygen Technologies Inc, Beijing, China) with the classic GOD-POD method [37, 38]. The assay was performed according to the manufacturer's instructions. Briefly, 5 μL of mediums and Glucose Standard were added into a 96-well plate, followed by the addition of 195 μL of the reaction solution.

The plate was incubated at 37 °C for 20 min. The glucose concentrations were determined by measuring the absorbance of the quinoneimine generated in the reaction at 570 nm. The glucose consumption of each compound was obtained by subtracting the glucose level in the medium, and represented as the percentage of the DMSO vehicle group.

4.2.4 Mitochondria complex I activity assay

Mitochondria complex I activity was measured by a sensitive and accurate commercial kit (MitoTox^{TM} Complex I OXPHOS Activity Assay Kit, ab109903, Abcam). The assay was performed strictly following the manufacturer's instructions. Briefly, the bovine heart mitochondria dissolved in a detergent was plated into a 96-well plate (coated with the complex I specific antibody) for 2 h at room temperature. Then the phospholipids were added to the plates, followed by the addition of the mixtures of the complex I solution and the test compounds, the positive control Rotenone, or the vehicle control DMSO. The reaction progression was monitored by following the oxidation of NADH as a decrease in absorbance at OD 340 nm. The output at OD 340 nm on the microplate reader was measured in kinetic mode, every minute, for at least 2 hours at 30 °C. The complex I activity was proportional to the decrease in absorbance at OD 340 nm.

4.2.5 Metabolic stability

Metabolic stability of compounds in mouse (ICR/CD-1) and human liver microsomes was assessed by Shanghai Medicilon Inc. (Shanghai, China). Briefly, the preheated potassium phosphate buffer containing compound (**B10** or **B4**) and liver microsomes were added into the assay plates and kept at 37 °C for 5 minutes. NADPH was then added to the plates to start the reaction. After specific time points (0 min, 5 min, 15 min, 30 min, 45 min), acetonitrile containing internal standard (Tolbutamide) was added to stop the reaction. After quenching and centrifuging at 6000 rpm for 15 min, supernatants were collected and subjected to LC/MS analysis.

4.2.6 Glucose tolerance test

All animal studies were conducted in accordance with the guiding principles of Animal Care and Use Committee of the China Pharmaceutical University (Nanjing, China).

C57BL/6 mice (male, 8-week old) were purchased from Beijing Vital River Laboratory Animal Technology Co., Ltd. (Beijing, China). Mice were housed under standard conditions with light/ dark cycle of 12 h. For glucose tolerance tests (ipGTT), mice were randomly grouped and fasted for 6 h, followed by intragastric administration of compounds or vehicle. At 2 h post treatment, mice were intraperitoneally injected with 20% (w/v) glucose (2 g/kg). Blood glucose in the tail vein blood were measured using glucometer (Accu-Chek, Roche, Nutley, NJ) at -120 (prior to compound treatment), 0 (prior to glucose administration), 20, 40, 60, 90 min post glucose administration. Area under the curve (AUC) of glucose time curve was estimated and net AUC was calculated after subtracting the AUC of no glucose challenge control group or not.

4.2.7 Hypoglycemic study in db/db mice

db/db mice (5-week old) were grouped to obtain similar average baseline blood glucose and body weight. The three grouped mice were as follows: db/db-veh (0.5% methylcellulose), db/db-**B10** (**B10**, 100 mg/kg/day), and non-diabetic control, db/m-veh (0.5% methylcellulose). Body weight and fasting blood glucose were measured weekly. For insulin tolerance tests, db/db mice were intraperitoneally injected with insulin (1.5 mU insulin per g of body weight) after being fasted for 6 h. Subsequently, mice were tail bled for measurement of blood glucose levels.

4.2.8 Cardiac safety study

C57BL/6 mice (male, 9-week old) were intragastrically received with **B10** (100 mg/kg), MK-8722 (10 mg/kg) or vehicle control daily for 4 weeks. At the end of experiment, animals were euthanized and perfused with saline. Organs weight and tibia length were recorded. Gross morphology of hearts from each group were randomly selected based on their similar body weight. Heart pieces were embedded in

paraffin after being fixed in 4% (weight/volume) paraformaldehyde, and then stained with periodic acid-Schiff (PAS) for glycogen staining.

4.2.9 Statistical analysis

All *in vitro* experiments data are presented as the means ± SD and *in vivo* experiments data are presented as the means ± SEM. The differences between two groups were determined by Student's *t*-test and means between multiple groups were compared using two-way ANOVA with Turkey's multiple comparisons test. $P < 0.05$ were considered statistically significant.

Declaration of competing interest

The authors declare no competing financial interest.

Acknowledgement

Financial support from the National Natural Science Foundation of China (21977118 and 81773584) is gratefully acknowledged. This research was also supported by the Jiangsu Provincial Key Research and Development Project (BE2018710), the National Science & Technology Major Project "Key New Drug Creation and Manufacturing Program", China (2019ZX09201001-003-004 and 2019ZX09301-151), the "Double First-Class" University Project (CPU2018GY01) and the BAGUI Scholar Program of Guangxi Province of China (2016A13).

Supplementary data

Supplementary data to this article can be found online.

References

1. F.A. Ross, C. MacKintosh, and D.G. Hardie, Amp-activated protein kinase: A cellular energy sensor that comes in 12 flavours. FEBS J. 283(16) (2016) 2987-3001.

2. M. Li, C.S. Zhang, Y. Zong, J.W. Feng, T. Ma, M. Hu, et al., Transient receptor potential v channels are essential for glucose sensing by aldolase and ampk. Cell

Metab. 30(3) (2019) 508-524 e512.

3. S.P. Davies, S.A. Hawley, A. Woods, D. Carling, T.A. Haystead, and D.G. Hardie, Purification of the amp-activated protein kinase on atp-gamma-sepharose and analysis of its subunit structure. Eur J Biochem. 223(2) (1994) 351-357.

4. L. Chen, Q. Chen, P. Rong, H.Y. Wang, and S. Chen, The energy sensing lkb1-ampkalpha1 pathway regulates igf1 secretion and consequent activation of the igf1r-pkb pathway in primary hepatocytes. FEBS J. 284(13) (2017) 2096-2109.

5. Y. Fujiwara, Y. Hiraoka, T. Fujimoto, N. Kanayama, M. Magari, and H. Tokumitsu, Analysis of distinct roles of camkk isoforms using sto-609-resistant mutants in living cells. Biochemistry. 54(25) (2015) 3969-3977.

6. S.A. Hawley, D.A. Pan, K.J. Mustard, L. Ross, J. Bain, A.M. Edelman, et al., Calmodulin-dependent protein kinase kinase-beta is an alternative upstream kinase for amp-activated protein kinase. Cell Metab. 2(1) (2005) 9-19.

7. K.O. Cameron, D.W. Kung, A.S. Kalgutkar, R.G. Kurumbail, R. Miller, C.T. Salatto, et al., Discovery and preclinical characterization of 6-chloro-5-[4-(1-hydroxycyclobutyl)phenyl]-1h-indole-3-carboxylic acid (pf-06409577), a direct activator of adenosine monophosphate-activated protein kinase (ampk), for the potential treatment of diabetic nephropathy. J Med Chem. 59(17) (2016) 8068-8081.

8. D.G. Hardie, Ampk: A target for drugs and natural products with effects on both diabetes and cancer. Diabetes. 62(7) (2013) 2164-2172.

9. M. Suter, U. Riek, R. Tuerk, U. Schlattner, T. Wallimann, and D. Neumann, Dissecting

the role of 5'-amp for allosteric stimulation, activation, and deactivation of amp-activated protein kinase. The Journal of biological chemistry. 281(43) (2006) 32207-32216.

10. K.A. Coughlan, R.J. Valentine, N.B. Ruderman, and A.K. Saha, Ampk activation: A therapeutic target for type 2 diabetes? Diabetes Metab Syndr Obes. 7 (2014) 241-253.

11. S. Zhou, Y. Duan, J. Wang, J. Zhang, H. Sun, H. Jiang, et al., Design, synthesis and biological evaluation of 4,7,12,12a-tetrahydro-5h-thieno[3',2':3,4]pyrido[1,2-b]isoquinolines as novel adenosine 5'-monophosphate-activated protein kinase (ampk) indirect activators for the treatment of type 2 diabetes. Eur J Med Chem. 140 (2017) 448-464.

12. Y.D. Kim, K.G. Park, Y.S. Lee, Y.Y. Park, D.K. Kim, B. Nedumaran, et al., Metformin inhibits hepatic gluconeogenesis through amp-activated protein kinase-dependent regulation of the orphan nuclear receptor shp. Diabetes. 57(2) (2008) 306-314.

13. G. Zhou, R. Myers, Y. Li, Y. Chen, X. Shen, J. Fenyk-Melody, et al., Role of amp-activated protein kinase in mechanism of metformin action. J Clin Invest. 108(8) (2001) 1167-1174.

14. D.G. Hardie, F.A. Ross, and S.A. Hawley, Ampk: A nutrient and energy sensor that maintains energy homeostasis. Nat Rev Mol Cell Biol. 13(4) (2012) 251-262.

15. J. Kirchner, B. Brune, and D. Namgaladze, Aicar inhibits nfkappab DNA binding independently of ampk to attenuate lps-triggered inflammatory responses in human macrophages. Sci Rep. 8(1) (2018) 7801.

16. E.C. Cokorinos, J. Delmore, A.R. Reyes, B. Albuquerque, R. Kjobsted, N.O.

Jorgensen, et al., Activation of skeletal muscle ampk promotes glucose disposal and glucose lowering in non-human primates and mice. Cell Metab. 25(5) (2017) 1147-1159 e1110.

17. R.W. Myers, H.P. Guan, J. Ehrhart, A. Petrov, S. Prahalada, E. Tozzo, et al., Systemic pan-ampk activator mk-8722 improves glucose homeostasis but induces cardiac hypertrophy. Science. 357(6350) (2017) 507-511.

18. Y. Jenkins, T.Q. Sun, V. Markovtsov, M. Foretz, W. Li, H. Nguyen, et al., Ampk activation through mitochondrial regulation results in increased substrate oxidation and improved metabolic parameters in models of diabetes. PloS one. 8(12) (2013) e81870.

19. Y. Huang, G. Sun, P. Wang, R. Shi, Y. Zhang, X. Wen, et al., Synthesis and biological evaluation of complex i inhibitor r419 and its derivatives as anticancer agents in hepg2 cells. Bioorg Med Chem Lett. 28(17) (2018) 2957-2960.

20. M.R. Owen, E. Doran, and A.P. Halestrap, Evidence that metformin exerts its anti-diabetic effects through inhibition of complex 1 of the mitochondrial respiratory chain. Biochem J. 348 Pt 3 (2000) 607-614.

21. B. Brunmair, K. Staniek, F. Gras, N. Scharf, A. Althaym, R. Clara, et al., Thiazolidinediones, like metformin, inhibit respiratory complex i: A common mechanism contributing to their antidiabetic actions? Diabetes. 53(4) (2004) 1052-1059.

22. N. Turner, J.Y. Li, A. Gosby, S.W. To, Z. Cheng, H. Miyoshi, et al., Berberine and its more biologically available derivative, dihydroberberine, inhibit mitochondrial

respiratory complex i: A mechanism for the action of berberine to activate amp-activated protein kinase and improve insulin action. Diabetes. 57(5) (2008) 1414-1418.

23. S. Vecchio, A. Giampreti, V.M. Petrolini, D. Lonati, A. Protti, P. Papa, et al., Metformin accumulation: Lactic acidosis and high plasmatic metformin levels in a retrospective case series of 66 patients on chronic therapy. Clin Toxicol (Phila). 52(2) (2014) 129-135.

24. E.P. Brass and C.L. Hoppel, Mitochondria as targets of drug toxicity: Lessons from the r118 phase i experience. Clin Pharmacol Ther. 98(5) (2015) 464-466.

25. T. Yamauchi, J. Kamon, Y. Ito, A. Tsuchida, T. Yokomizo, S. Kita, et al., Cloning of adiponectin receptors that mediate antidiabetic metabolic effects. Nature. 423(6941) (2003) 762-769.

26. T. Yamauchi, J. Kamon, Y. Minokoshi, Y. Ito, H. Waki, S. Uchida, et al., Adiponectin stimulates glucose utilization and fatty-acid oxidation by activating amp-activated protein kinase. Nature Medicine. 8(11) (2002) 1288-1295.

27. T. Yamauchi, Y. Nio, T. Maki, M. Kobayashi, T. Takazawa, M. Iwabu, et al., Targeted disruption of adipor1 and adipor2 causes abrogation of adiponectin binding and metabolic actions. Nature Medicine. 13(3) (2007) 332-339.

28. L. Otvos, Jr., I. Kovalszky, J. Olah, R. Coroniti, D. Knappe, F.I. Nollmann, et al., Optimization of adiponectin-derived peptides for inhibition of cancer cell growth and signaling. Biopolymers. 104(3) (2015) 156-166.

29. M. Okada-Iwabu, T. Yamauchi, M. Iwabu, T. Honma, K. Hamagami, K. Matsuda, et al.,

A small-molecule adipor agonist for type 2 diabetes and short life in obesity. Nature. 503(7477) (2013) 493-499.

30. M. Okada-Iwabu, M. Iwabu, K. Ueki, T. Yamauchi, and T. Kadowaki, Perspective of small-molecule adipor agonist for type 2 diabetes and short life in obesity. Diabetes Metab J. 39(5) (2015) 363-372.

31. M. Akimoto, R. Maruyama, Y. Kawabata, Y. Tajima, and K. Takenaga, Antidiabetic adiponectin receptor agonist adiporon suppresses tumour growth of pancreatic cancer by inducing ripk1/erk-dependent necroptosis. Cell Death Dis. 9(8) (2018) 804.

32. A.K. Singh, A.A. Joharapurkar, M.P. Khan, J.S. Mishra, N. Singh, M. Yadav, et al., Orally active osteoanabolic agent gtdf binds to adiponectin receptors, with a preference for adipor1, induces adiponectin-associated signaling, and improves metabolic health in a rodent model of diabetes. Diabetes. 63(10) (2014) 3530-3544.

33. B. Xiao, M.J. Sanders, D. Carmena, N.J. Bright, L.F. Haire, E. Underwood, et al., Structural basis of ampk regulation by small molecule activators. Nat Commun. 4 (2013) 3017.

34. H.L. Liu, J. Wang, D.Z. Lin, and H. Liu, Lead compound optimization strategy (2)--structure optimization strategy for reducing toxicity risks in drug design. Yao Xue Xue Bao. 49(1) (2014) 1-15.

35. E.Q. Li, W. Zhao, C.X. Zhang, L.Z. Qin, S.J. Liu, Z.Q. Feng, et al., Synthesis and anti-cancer activity of nd-646 and its derivatives as acetyl-coa carboxylase 1 inhibitors. Eur J Pharm Sci. 137 (2019).

36. C.P. Chen, K. Chen, Z. Feng, X. Wen, and H. Sun, Synergistic antitumor activity of

artesunate and hdac inhibitors through elevating heme synthesis via synergistic upregulation of alas1 expression. Acta Pharm Sin B. 9(5) (2019) 937-951.

37. P. Trinder, Determination of blood glucose using an oxidase-peroxidase system with a non-carcinogenic chromogen. J Clin Pathol. 22(2) (1969) 158-161.

38. D. Barham and P. Trinder, An improved colour reagent for the determination of blood glucose by the oxidase system. Analyst. 97(151) (1972) 142-145.

Highlights

- A series of novel AdipoRon analogues were designed and synthesized.
- Six analogues exhibited much more potency of AMPK activation than AdipoRon.
- **B10** exhibited significant *in vitro* and *in vivo* hypoglycemic effects in mice.
- **B10** did not inhibit mitochondrial complex I.
- **B10** did not cause cardiac hypertrophy in mice.

Declaration of interests

☒ The authors declare that they have no known competing financial interests or personal relationships that could have appeared to influence the work reported in this paper.

☐The authors declare the following financial interests/personal relationships which may be considered as potential competing interests: